

HERON contains contributions based mainly on research work performed in I.B.B.C. and STEVIN and related to strength of materials and structures and materials science.

HERON

vol. 23
1978
no. 4

Contents

BUCKLING STRENGTH OF PLYWOOD RESULTS OF TESTS AND DESIGN RECOMMENDATIONS

Ir. J. Dekker, Ir. J. Kuipers and Ir. H. Ploos van Amstel

Jointly edited by:

STEVIN-LABORATORY
of the Department of
Civil Engineering of the
Delft University of Technology,
Delft, The Netherlands
and
I.B.B.C. INSTITUTE TNO
for Building Materials
and Building Structures,
Rijswijk (ZH), The Netherlands.

EDITORIAL STAFF:

F. K. Ligtenberg, *editor in chief*
M. Dragosavić
H. W. Reinhardt
J. Strating
A. C. W. M. Vrouwenvelder
J. Witteveen

Secretariat:

L. van Zetten
P.O. Box 49
2600 AA Delft, The Netherlands

Summary	3
1 The investigation	5
1.1 Object	5
1.2 Theory	5
1.3 Test program	7
2 Test results	12
2.1 Stiffness properties	12
2.2 Buckling tests	15
2.2.1 General remarks	15
2.2.2 Determination of the critical stresses	15
3 Discussion of the results	18
4 Conclusions	30
5 Recommendations for design	32
5.1 Theoretical values for various loading conditions	32
5.1.1 Normal stresses	32
5.1.2 Shear stresses	35
5.1.3 Combinations of bending or normal stresses with shear	35
5.1.4 Combination of normal stresses in two directions (uniformly distributed)	38
5.1.5 Combination of two normal and shear stresses	38
6 Aspects of safety	39
References	41
Appendices	42

Publications in HERON since 1970

BUCKLING STRENGTH OF PLYWOOD

Results of tests and design recommendations

Summary

Tests were carried out on 100 specimens of Canadian Douglas fir plywood to verify that reasonably good agreement exists between the buckling theories and the actual behaviour of plywood. From load-deflection curves values for a critical buckling strength can be determined, which are in good agreement with theoretical values in the case of simply-supported edges. A clamped boundary condition could not be realised in such a way that the theoretical values were approximated. For design purposes this condition should not be presumed.

Attention has been paid to combinations of normal and shear stresses on the basis of theoretical considerations. This leads to proposals for the scope of design recommendations, which have not been worked out in detail here.

Buckling strength of plywood

Results of tests and design recommendations

1 The investigation

1.1 Object

The object of the investigation is to verify that plywood follows the usual buckling theories and that the use of the various mechanical properties as laid down in design codes leads to sufficient accuracy, or in any case to a sufficient degree of safety, in the prediction of the buckling strength.

A further aim of the investigation is to deduce safe design rules for structures and structural components, where plywood is loaded in compression and/or shear in its own plane.

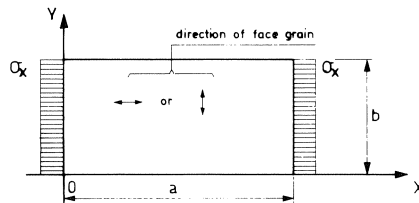


Fig. 1.

1.2 Theory

Plywood is assumed to behave like an orthotropic linear elastic material.

On the basis of the differential equation of the rectangular orthotropic plate together with an assumed plane after buckling an equilibrium state can be found if such a plate is loaded in its own plane, subject to certain boundary conditions along its edges.

If for a rectangular plate, simply-supported along its four edges, the curved surface after buckling is

$$w = A_{mn} \sin \frac{m\pi}{a} x \sin \frac{n\pi}{b} y,$$

the smallest value of the stress σ_x in Fig. 1, necessary to accomplish this equilibrium state, is found to be

$$\sigma_{xcr} = \frac{4\pi^2}{b^2 t} \left(N_x \frac{m^2 b^2}{4a^2} + N_{xy} \frac{n^2}{2} + N_y \frac{n^4 a^2}{4m^2 b^2} \right)$$

where

$$N_x = \frac{E_x t^3}{12(1-\nu_x \nu_y)}; \quad N_y = \frac{E_y t^3}{12(1-\nu_x \nu_y)}; \quad N_{xy} = \frac{1}{2} G I_w + \frac{1}{2} (\nu_x N_y + \nu_y N_x)$$

and where m and n are the number of half-waves in the X - and Y -direction respectively. If

$$\frac{a}{b} = \alpha; \quad \alpha_v = \alpha \sqrt[4]{\frac{N_y}{N_x}}; \quad \eta = \frac{N_{xy}}{\sqrt{N_x N_y}}$$

the formula for the critical stress becomes

$$\sigma_{scr} = \frac{4\pi^2}{b^2 t} \sqrt{N_x N_y} \left(\frac{m^2}{4\alpha_v^2} + \frac{1}{2} \eta n^2 + \frac{n^4 \alpha_v^2}{4m^2} \right) = K \frac{4\pi^2}{b^2 t} \sqrt{N_x N_y}$$

where K = "buckling factor".

Generally in the non-loaded Y -direction of the plate only one half-wave will develop; in that case $n = 1$ and

$$K = \frac{m^2}{4\alpha_v^2} + \frac{n}{2} + \frac{\alpha_v^2}{4m^2}$$

Values of K are given in Fig. 2.

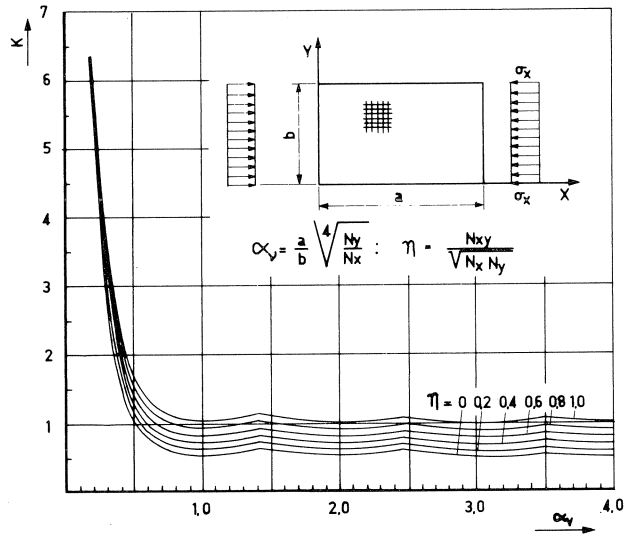


Fig. 2. Values of K for plates with all edges simply supported [3].
(Numbers in [...] refer to literature listed).

For rectangular plates with clamped edges in the X -direction Lekhnitskii has given a solution from which follows a critical stress ($n = 1$)

$$\sigma_{cr} = \frac{4\pi^2}{b^2 t} \sqrt{N_x N_y} \left(\frac{m^2}{4\alpha_v^2} + \frac{2}{3} \eta + \frac{4}{3} \frac{\alpha_v^2}{m^2} \right) = K \frac{4\pi^2}{b^2 t} \sqrt{N_x N_y}$$

For this case values of

$$K = \frac{m^2}{4\alpha_v^2} + \frac{2\eta_l}{3} + \frac{4\alpha_v^2}{3m^2}$$

are given in Fig. 3.

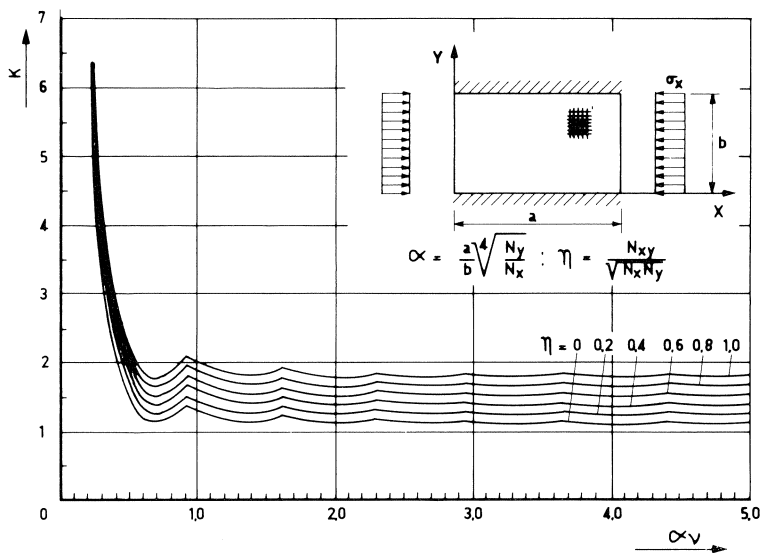


Fig. 3. Values of K for plates with edges // X -axis clamped; the edges // Y -axis are simply-supported [3].

1.3 Test program

To control the validity of the theories for plywood, specimens of two thicknesses (8 resp. 13 mm) and of different dimensions were tested. Data of the test program are given in Table 1.

Table 1. Test program.

b mm		$\alpha = a/b$ (see Fig. 1)	number of variables
400	tests // grain $\rightarrow \sigma_{//}$	$1/2$ 1 $1\frac{1}{2}$ 2 $2\frac{1}{2}$ 3 $3\frac{1}{2}$ 4 $4\frac{1}{2}$	9
	tests \perp grain $\rightarrow \sigma_{\perp}$	$1/2$ 1 $1\frac{1}{2}$ 2 $2\frac{1}{2}$ 3 $3\frac{1}{2}$ 4 $4\frac{1}{2}$	6
600	tests // grain $\rightarrow \sigma_{//}$	$1/2$ 1 $1\frac{1}{2}$ 2 $2\frac{1}{2}$ 3 - - -	6
	tests \perp grain $\rightarrow \sigma_{\perp}$	$1/2$ 1 $1\frac{1}{2}$ 2 - - - -	4
			25

Each test specimen was made in two thicknesses - 8 and 13 mm - and furthermore two kinds of support were used: simply-supported at all edges, and clamped edges in the X -

direction combined with simply-supported edges in the Y -direction. In this way $25 \times 2 \times 2 = 100$ buckling tests were done.

In all cases Canadian Douglas fir plywood, of the quality Select Sheathing, Ext. 1, was used. The test specimens were stored in the unconditioned laboratory hall for several months; the moisture content at test was 8 to 10%.

From each test specimen the thickness t , the length a and the width b were measured, furthermore the stiffness properties

$$N_x = \frac{E_x t^3}{12(1-\nu_x \nu_y)}; \quad N_y = \frac{E_y t^3}{12(1-\nu_x \nu_y)}$$

and

$$N_{xy} = \frac{1}{2}GI_w + \frac{1}{2}(\nu_x N_y + \nu_y N_x) \approx \frac{1}{6}Gt^3$$

were determined.

With these quantities the values of the governing factors

$$\alpha_v = \alpha \sqrt[4]{\frac{N_y}{N_x}} \quad \text{and} \quad \eta_l = \frac{N_{xy}}{\sqrt{N_x N_y}}$$

for all single panels could be calculated, as well as the critical stresses.

1.4 Test set-up

All bending tests to determine values of N_x and N_y were carried out by direct loading of the individual panels and measuring the deflections (see photographs).

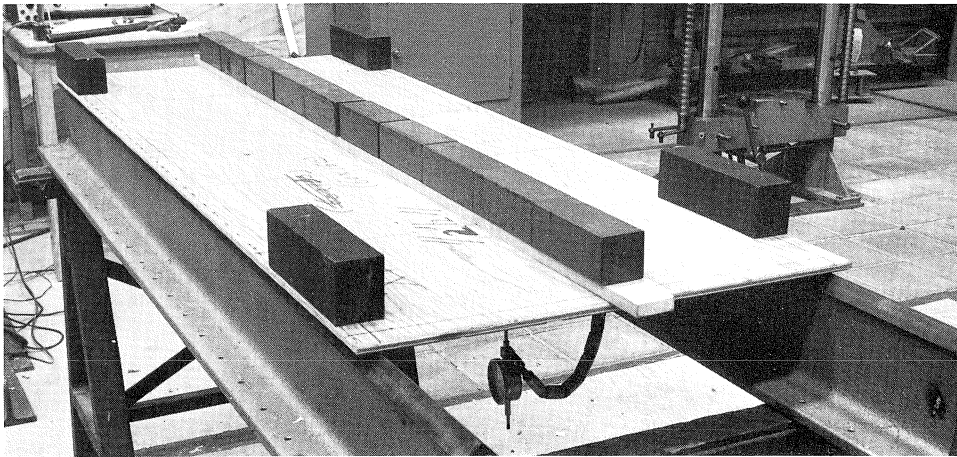
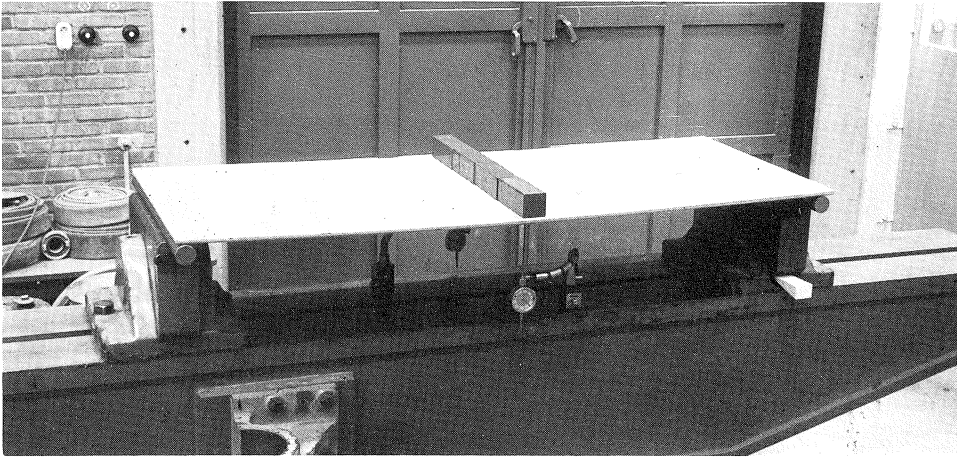
N_{xy} was determined by a four-point loading system according to Nadai (Fig. 4), from which can be calculated

$$G = \frac{3l_1 l_2 F}{wt^3}, \quad \text{and hence } N_{xy} = \frac{1}{6}Gt^3.$$

Especially in these tests only small loads and deformations were used to achieve sufficient accuracy.

In order to avoid too great differences between l_1 and l_2 , N_{xy} could only be determined for the square test panels in the program. For the other test panels N_{xy} had to be determined for representative parts of the whole plywood panel of which the test specimens were made.

The buckling tests were carried out in a specially designed frame. The set-up and some details are given in Fig. 5. The load was applied by a hydraulic jack and transmitted via a balanced beam to two blocks with a V-groove, in which the panel rested. A similar



Bending tests for the determination of N_x and N_y .

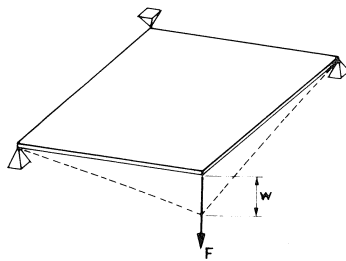


Fig. 4.

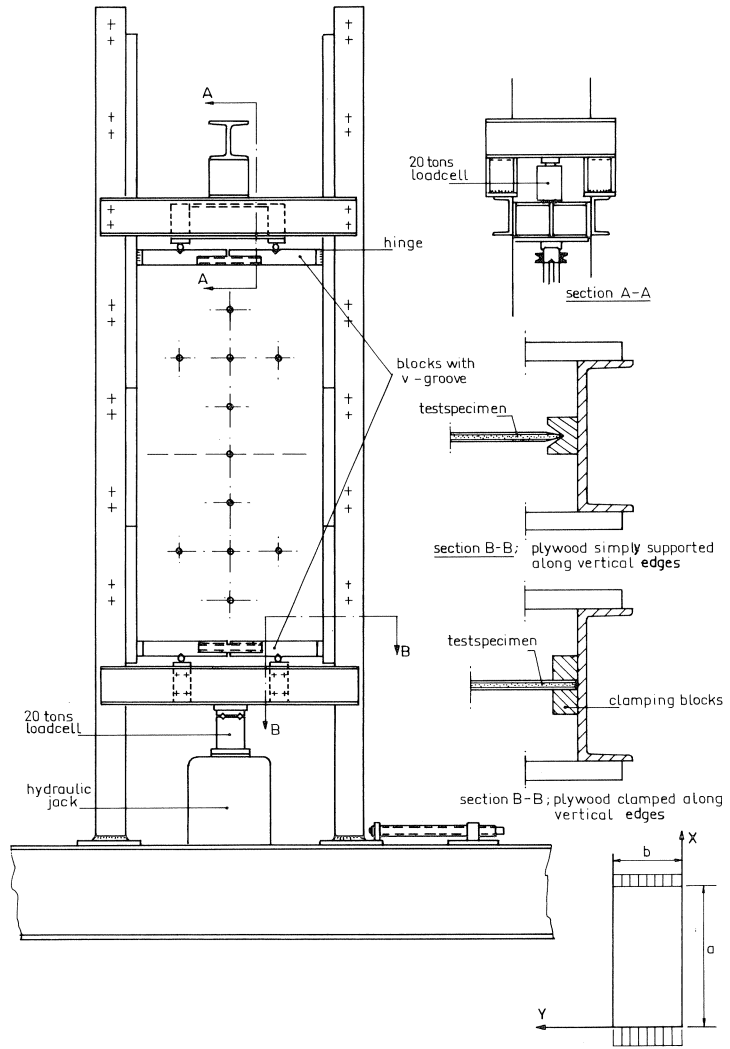


Fig. 5.

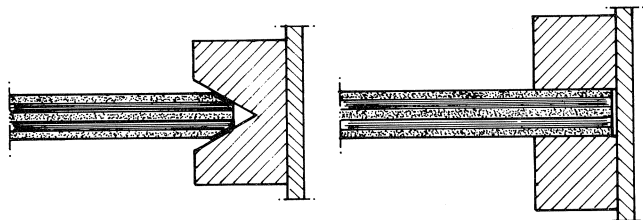
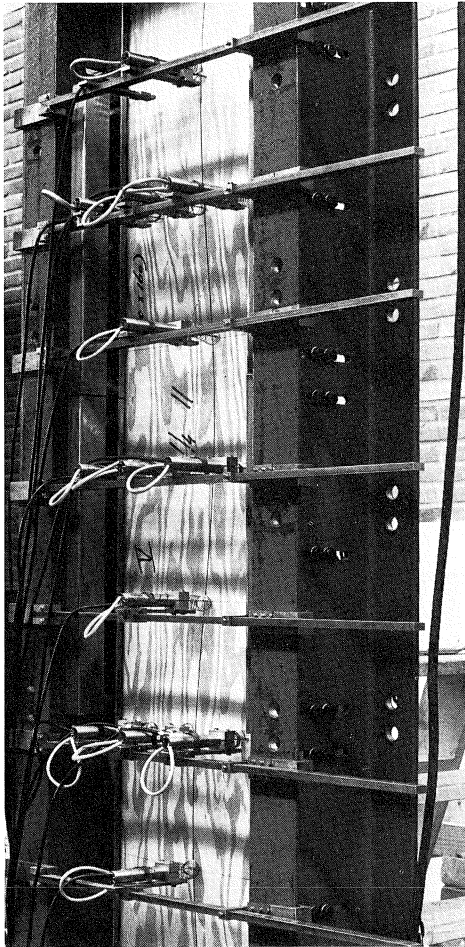


Fig. 6.



Simply-supported test specimens, loaded parallel to direction of face grain.
 $\alpha = 4$; 3 halfwaves.



Test specimen with clamped vertical edges. Face veneer horizontal, i.e., perpendicular to the direction of the load.
 $\alpha = 3$; 4 halfwaves.

arrangement was used at the upper edge. At the directly loaded lower edge and at the upper edge the load and the reaction force were respectively measured, a difference being possible due to friction along the edges of the panel.

For the simply-supported panels the side members of the frame in the X -direction had a V-groove for holding somewhat tapered panel edges. The panels to be tested with clamped edges in two X -direction were held between steel clamping blocks tightened with screw-clamps.

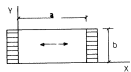
Depending on the dimensions of the panels, the deflections normal to the plane were measured at several places by inductive displacement transducers (see photographs).

2 Test results

2.1 Stiffness properties

Tables 2 to 5 give values of N_x , N_y and N_{xy} for the test specimens. Mean values obtained from all these panels are given in Table 6.

Table 2. Stiffness properties; α_v - and η -values. Simply-supported panels loaded // grain of face veneers

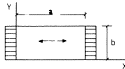
			α								
			1/2	1	1 1/2	2	2 1/2	3	3 1/2	4	4 1/2
400	8	t (mm)	8,15	8,10	7,83	8,15	7,95	7,98	8,03	8,00	8,15
		N_x	170	315	424	697	579	593	524	780	834
		N_y	79	43	94	89	94	90	98	96	95
		N_{xy}	68	77	63	77	78	77	63	77	77
		α_v	0,41	0,61	1,03	1,19	1,59	1,87	2,30	2,37	2,61
	η	0,59	0,66	0,32	0,31	0,33	0,33	0,28	0,28	0,27	
	13	t (mm)	12,1	12,0	12,0	11,9	11,9	11,9	12,2	11,9	12,0
		N_x	911	915	1705	1846	1838	1818	1819	1925	2095
		N_y	580	479	528	439	492	362	522	404	451
		N_{xy}	206	228	229	206	206	206	229	206	206
α_v		0,45	0,85	1,12	1,39	1,80	2,00	2,56	2,71	3,07	
η	0,28	0,34	0,24	0,23	0,23	0,25	0,24	0,23	0,21		
600	8	t (mm)	7,45	8,48	7,56	7,55	7,58	7,51			
		N_x	434	455	535	581	584	538			
		N_y	39	34	40	39	32	37			
		N_{xy}	73	71	54	54	73	73			
		α_v	0,28	0,52	0,79	1,02	1,21	1,53			
	η	0,56	0,57	0,37	0,36	0,53	0,52				
	13	t (mm)	12,3	12,2	12,2	12,2	12,2	12,2			
		N_x	1176	1698	1613	1472	1838	1937			
		N_y	371	491	472	536	434	432			
		N_{xy}	245	248	272	272	245	245			
α_v		0,38	0,73	1,10	1,55	1,74	2,06				
η	0,37	0,27	0,31	0,31	0,27	0,27					

¹ N_x and N_y are determined for each specimen separately; N_{xy} sometimes was determined for the plywood panel from which the specimens were taken.

² N_x , N_y and N_{xy} in kN mm²/mm.

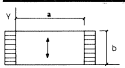
³ The values of N_x and N_y show great differences, especially if α is small. This can partly be ascribed to the fact that the E -values were measured in a 3-point bending test in which the load had a relatively great length compared with the span (resp. 50 mm and 160 mm).

Table 3. Stiffness properties; α_v - and η -values. Panels with clamped edges in X -direction loaded // grain of face veneers



			α									
			1/2	1	1 1/2	2	2 1/2	3	3 1/2	4	4 1/2	
400	8	t (mm)	7,95	7,85	8,21	7,98	8,47	7,83	7,95	7,85	8,05	
		N_x	241	501	436	449	496	437	487	748	549	
		N_y	91	62	81	72	76	67	64	71	78	
		N_{xy}	95	59	95	57	55	57	93	94	93	
		α_v	0,39	0,59	0,98	1,27	1,56	1,87	2,10	2,22	2,76	
		η	0,61	0,33	0,51	0,32	0,28	0,33	0,53	0,41	0,45	
	13	t (mm)	12,2	12,0	12,2	12,7	12,0	12,6	12,3	12,0	12,2	
		N_x	765	1069	2448	1891	1420	1875	2261	2555	2155	
		N_y	603	467	660	729	620	640	591	377	572	
		N_{xy}	289	184	289	233	180	238	306	206	306	
		α_v	0,47	0,81	1,08	1,58	2,03	2,29	2,50	2,48	3,23	
		η	0,43	0,26	0,23	0,20	0,19	0,22	0,26	0,21	0,28	
	600	8	t (mm)	7,58	7,85	8,44	7,85	7,86	7,90			
			N_x	269	502	461	177	474	568			
N_y			73	67	79	82	82	95				
N_{xy}			85	91	55	94	85	91				
α_v			0,26	0,60	0,96	1,65	1,61	1,91				
η			0,61	0,50	0,29	0,78	0,43	0,39				
13		t (mm)	12,0	12,0	12,0	12,0	12,1	12,0				
		N_x	645	1435	1072	1698	1409	1810				
		N_y	640	474	601	384	620	480				
		N_{xy}	183	177	183	206	183	177				
		α_v	0,50	0,75	1,29	1,38	2,0	2,15				
		η	0,28	0,21	0,23	0,26	0,20	0,19				

Table 4. Stiffness properties; α_v - and η -values. Simply-supported panels loaded \perp grain of face veneers



			α									
			1/2	1	1 1/2	2	2 1/2	3	3 1/2	4	4 1/2	
400	8	t (mm)	7,58	7,63	7,75	7,73	7,80	7,98				
		N_x	73	102	92	95	107	117				
		N_y	349	382	348	328	328	375				
		N_{xy}	53	63	63	63	63	63				
		α_v	0,73	1,39	2,09	2,71	3,30	4,01				
		η	0,33	0,32	0,35	0,36	0,34	0,30				
	13	t (mm)	12,1	12,0	12,2	12,3	12,3	12,4				
		N_x	354	523	530	498	557	559				
		N_y	1567	1207	1464	1356	1276	950				
		N_{xy}	229	259	229	229	229	229				
		α_v	0,72	1,23	1,93	2,56	3,08	3,43				
		η	0,31	0,33	0,26	0,28	0,27	0,31				
	600	8	t (mm)	7,43	8,49	7,54	7,53					
			N_x	53	40	41	43					
N_y			524	551	494	575						
N_{xy}			54	74	54	54						
α_v			0,89	1,92	2,78	3,3						
η			0,32	0,50	0,38	0,34						
13		t (mm)	12,4	12,4	12,4	12,3						
		N_x	429	418	579	515						
		N_y	1247	1524	1569	1497						
		N_{xy}	272	242	272	272						
		α_v	0,65	1,38	1,92	2,91						
		η	0,37	0,30	0,29	0,31						

Table 5. Stiffness properties; α_v - and η -values. Panels with clamped edges in X -direction loaded \perp grain of face veneers

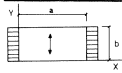
			α								
			$1/2$	1	$1\frac{1}{2}$	2	$2\frac{1}{2}$	3	$3\frac{1}{2}$	4	$4\frac{1}{2}$
400	8	t (mm)	7,95	7,85	7,95	7,90		7,83			
		N_x	63	102	98	82		116			
		N_y	429	461	423	351		368			
		N_{xy}	91	71	91	57		57			
		α_v	0,81	1,46	2,16	3,63		4,00			
		η	0,55	0,33	0,45	0,34		0,28			
13	8	t (mm)	12,6	12,0	12,3	12,8		12,6			
		N_x	298	388	649	866		831			
		N_y	1422	1489	2420	1349		1702			
		N_{xy}	238	150	323	238		238			
		α_v	0,74	1,40	5,60	2,23		3,59			
		η	0,37	0,20	0,26	0,22		0,20			
600	8	t (mm)	7,75	7,85	7,80	7,73					
		N_x	75	61	83	119					
		N_y	312	493	401	425					
		N_{xy}	55	94	55	55					
		α_v	0,71	1,68	2,22	2,75					
		η	0,36	0,54	0,30	0,24					
13	8	t (mm)	12,0	12,1	12,0	12,0					
		N_x	372	470	698	650					
		N_y	1060	2950	928	999					
		N_{xy}	183	206	183	183					
		α_v	0,64	1,58	1,61	2,23					
		η	0,29	0,17	0,23	0,23					

Table 6. Mean values of $N_{//}$,* N_{\perp} * and N_{xy} (in $\text{kN mm}^2/\text{mm}$)

plywood t	$N_{//}$			N_{\perp}			N_{xy}		
	mean	stand. dev.	coeff. var.	mean	stand. dev.	coeff. var.	mean	stand. dev.	coeff. var.
8 mm	464	137	0,30	76	24	0,32	71	15	0,21
13 mm	1578	490	0,31	523	121	0,23	226	44	0,19

* In this table $N_{//}$ and N_{\perp} are used. In Tables 2 and 3: $N_{//} \equiv N_x$ and $N_{\perp} \equiv N_y$. In Table 4 and 5: $N_{//} \equiv N_y$ and $N_{\perp} \equiv N_x$.

The mean ratio $N_{//}/N_{\perp}$ is 6,1 for the 8 mm and 3,0 for the 13 mm plywood; this means that $\sqrt[4]{N_{//}/N_{\perp}} = 1,57$ and 1,33 respectively. The mean values of $N_{xy}/\sqrt{N_{//}N_{\perp}} = 0,67$ and 0,26 respectively. In the investigation the values of α and η were calculated for each panel individually and were used to predict the buckling strength; these values of α_v and η are also given in Tables 2 to 5.

2.2 Buckling tests

2.2.1 General remarks

During the first series of tests it was noticed that long test panels, showing more than one buckling half-wave, buckled first at the directly loaded edge. A second buckling half-wave occurred more to the reaction edge of the panel, for a higher load at the hydraulic jack (cf. Fig. 5), etc. After this had happened during the first series the second load cell at the reaction edge was placed.

In the following tests a varying difference between the loads at the lower and the upper edge was measured, this being due to the friction along the supported edges in X -direction. This difference has a tendency to grow with increasing length of the specimens, although the variance is too high to make this tendency significant. For individual test specimens the load at the upper edge ranged from $F_{up} = 0,96F_{low}$ to $F_{up} = 0,45F_{low}$.

These differences occurred at failure; before reaching this stage they were generally smaller.

It was shown that it is most probably not too unrealistic to assume that the normal stress σ_x in the panel varies linearly from σ_{low} to σ_{up} . It was therefore decided that "the" stress on the panel could be found as the mean value of σ_{low} and σ_{up} . Furthermore the critical stresses for the individual buckling half-waves were determined and the mean value thereof was given as the buckling stress for the panel.

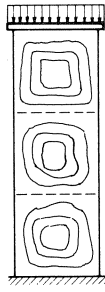


Fig. 7.

2.2.2 Determination of the critical stresses

The critical stresses themselves were determined from the measurements of the deformations. Examples of the relation between the stress and the displacements normal to the plane are given in Fig. 8.

It can clearly be seen that right from the beginning of the loading procedure the originally existing eccentricities* lead to increasing deformations, which after some time follow a nearly straight line. It is also clear that during the tests the deformation was

* Initial eccentricities were measured from $\frac{1}{2}$ to 9% from the shorter edge of the plywood panel.

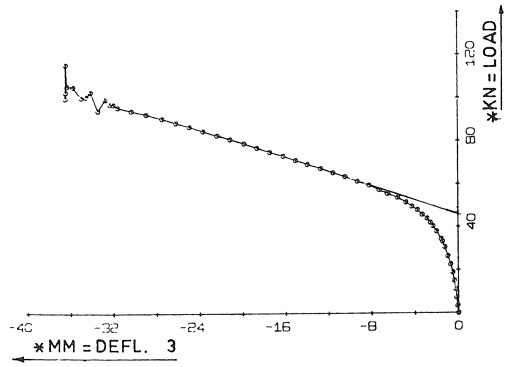
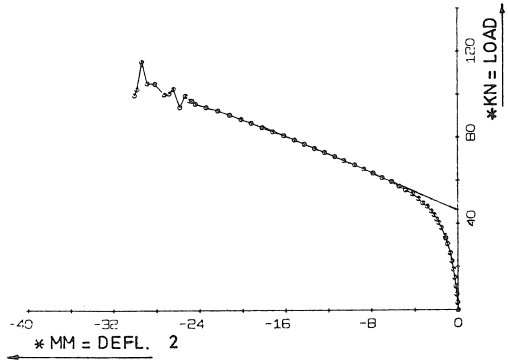
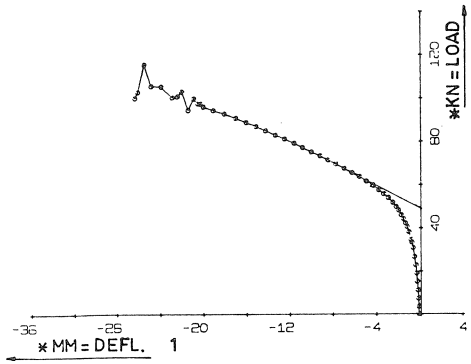


Fig. 8.

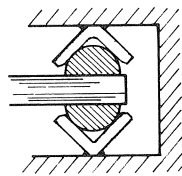


Fig. 9.

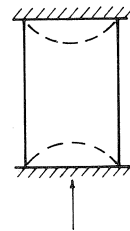


Fig. 10.

gradually increasing; there was no sign of a sudden occurrence of buckling as was found in the investigation described in [3]. This different behaviour could possibly be the effect of other boundary conditions. In [3] the “simple support” was constructed as shown in Fig. 9, where half-round laths were glued to the plywood. In the investigation described here such a simple support was constructed as shown in Figs. 5 and 6.

In most cases the failure load or ultimate load is much higher than the critical load. It must be added however, that this “post-buckling behaviour” was much more pronounced with longer plates than with shorter ones, and that this effect disappeared with the very short plates, where instead the compressive strength was the governing property.

In most cases the highest load caused failure in the plywood plate as in Fig. 10. The values of σ_{cr} and σ_{ult} are listed in Tables 7 to 10.

Table 7. Calculated values of σ_{cr} (in N/mm²) and test results. Simply-supported panels loaded // grain of face veneers.

			α										
				$\frac{1}{2}$	1	$1\frac{1}{2}$	2	$2\frac{1}{2}$	3	$3\frac{1}{2}$	4	$4\frac{1}{2}$	
8	calculated	TGH	α_v	0,25	0,5	0,75	1,00	1,25	1,50	1,75	2,00	2,25	
			σ_{cr}	11,6	3,79	2,44	2,23	2,36	2,44	2,25	2,23	2,25	
		measurements	α_v	0,41	0,61	1,03	1,19	1,59	1,87	2,30	2,37	2,61	
			σ_{cr}	6,37	3,95	4,15	5,21	5,20	4,76	4,58	5,63	5,59	
		test	σ_{cr}	13,37	8,21	4,58	7,15	4,81	6,96	3,88	5,11	3,94	
			σ_{ult}	15,1	12,3	11,3	18,0	11,2	16,1	11,3	12,8	10,3	
	400	calculated	TGH	α_v	0,38	0,75	1,13	1,50	1,88	2,25	2,63	3,00	3,38
				σ_{cr}	30,8	11,8	10,6	11,8	10,6	10,8	10,7	10,6	10,7
			measurements	α_v	0,45	0,85	1,12	1,39	1,80	2,00	2,56	2,71	3,07
				σ_{cr}	21,4	9,50	12,3	13,4	12,2	10,6	12,6	11,5	12,2
			test	σ_{cr}		15,4	11,6	14,6	14,9	10,4	11,6	10,5	12,2
				σ_{ult}	24,1	17,6	19,7	18,6	21,1	18,0	18,6	18,4	18,8
600		calculated	TGH	α_v	0,25	0,5	0,75	1,00	1,25	1,50			
				σ_{cr}	5,16	1,69	1,12	1,03	1,08	1,12			
			measurements	α_v	0,28	0,52	0,79	1,02	1,21	1,53			
				σ_{cr}	7,12	2,08	1,43	1,31	1,45	1,66			
			test	σ_{cr}	10,1	3,37	2,15	0,96	1,04	1,40			
				σ_{ult}	14,7	5,43	6,96	6,24	5,46	5,25			
	13	calculated	TGH	α_v	0,38	0,75	1,13	1,50	1,88	2,25			
				σ_{cr}	14,0	5,25	4,69	5,25	4,63	4,69			
		measurements	α_v	0,38	0,73	1,10	1,55	1,74	2,06				
			σ_{cr}	13,2	5,77	5,15	5,34	5,11	4,94				
		test	σ_{cr}	13,7	6,53	6,29	5,83	4,76	3,95				
			σ_{ult}	13,8	9,96	13,5	13,1	10,3	10,6				

Table 8. Calculated values of σ_{cr} and test results. Simply-supported panels loaded \perp grain of face veneers

				α											
				1/2	1	1 1/2	2	2 1/2	3	3 1/2	4	4 1/2			
400	8	calculated	TGH	α_v	1	2	3	4	5	6					
				σ_{cr}	2,23	2,23	2,23	2,23	2,23	2,23					
		test		σ_{cr}	6,53	5,96	3,91	4,62	3,53	4,19					
				σ_{ult}	8,40	9,54	9,13	9,88	9,74	10,4					
		13	calculated	TGH	α_v	0,67	1,34	2,01	2,68	3,35	4,02				
					σ_{cr}	13,1	11,8	10,6	10,6	10,6	10,4				
	test			σ_{cr}	14,4	14,9	13,0	12,7	11,8	11,4					
				σ_{ult}	17,4	18,7	15,6	17,9	15,6	16,5					
	600		8	calculated	TGH	α_v	1	2	3	4					
						σ_{cr}	1,03	1,03	1,03	1,03					
		test			σ_{cr}	0,89	1,92	2,78	3,3						
					σ_{cr}	1,43	1,59	1,33	1,4						
13		calculated		TGH	α_v	0,67	1,34	2,01	2,68						
					σ_{cr}	5,80	5,25	4,63	4,69						
		test		σ_{cr}	6,93	5,31	5,14	5,34							
				σ_{ult}	9,30	9,00	10,8	10,9							

3 Discussion of the test results

In the Tables 7 to 10 the first two lines for a certain type of panel are headed "TGH". Among other design information, the publication "TGH"* gives E and G -values for plywood.

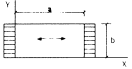
For 8 mm plywood it gives $E_{//} = 8000 \text{ N/mm}^2$

$$E_{\perp} = 500 \text{ N/mm}^2$$

$$G = 750 \text{ N/mm}^2$$

* "TGH" = "Tabellen en Grafieken voor Houtconstructies"
= Tables and graphs for timber structures; [7].

Table 9. Calculated values of σ_{cr} and test results. Panels with clamped edges in X -direction, loaded // grain of face veneers



				α									
				$1/2$	1	$1\frac{1}{2}$	2	$2\frac{1}{2}$	3	$3\frac{1}{2}$	4	$4\frac{1}{2}$	
400	8	calculated	TGH	α_v	0,25	0,5	0,75	1,00	1,25	1,50	1,75	2,00	2,25
				σ_{cr}	12,0	4,85	4,48	4,85	4,39	4,48	4,46	4,37	4,48
		measurements	α_v	0,39	0,59	0,98	1,27	1,56	1,87	2,10	2,22	2,76	
			σ_{cr}	10,5	7,80	9,58	7,54	7,94	7,42	8,28	10,6	9,22	
		test	σ_{cr}	10,1	7,39	4,98	8,07	5,28	4,79	4,75	5,81	5,59	
			σ_{ult}	12,8	13,9	14,7	10,2	11,5	11,2	14,2	15,9	13,8	
	13	calculated	TGH	α_v	0,38	0,75	1,13	1,50	1,88	2,25	2,63	3,00	3,38
				σ_{cr}	34,1	22,1	22,3	22,1	21,6	22,3	21,5	21,8	21,5
		measurements	α_v	0,47	0,81	1,08	1,58	2,03	2,29	2,50	2,48	3,23	
			σ_{cr}	23,4	22,8	35,9	31,1	24,7	28,9	30,9	26,3	30,2	
		test	σ_{cr}		14,4	7,52	13,9	10,0	13,7	15,1	13,9	13,9	
			σ_{ult}	25,7	21,4	26,3	22,5	20,5	21,1	26,1	28,5	25,3	
600	8	calculated	TGH	α_v	0,25	0,5	0,75	1,00	1,25	1,50	1,75	2,00	2,25
				σ_{cr}	3,88	1,68	1,57	1,68	1,48	1,52			
		measurements	α_v	0,26	0,60	0,96	1,65	1,61	1,91				
			σ_{cr}	4,91	3,83	3,91	2,93	4,24	4,58				
		test	σ_{cr}	4,76	3,27	2,79	3,14	2,67	3,20				
			σ_{ult}	6,68	10,4	8,50	9,10	10,6	8,32				
	13	calculated	TGH	α_v	0,38	0,75	1,13	1,50	1,88	2,25			
				σ_{cr}	14,2	8,54	8,66	8,54	8,30	8,54			
		measurements	α_v	0,50	0,75	1,29	1,38	2,00	2,15				
			σ_{cr}	8,93	10,1	9,59	9,80	10,9	11,1				
		test	σ_{cr}	8,86	5,42	6,35	5,82	5,56	6,68				
			σ_{ult}	11,7	13,3	11,6	15,4	12,3	13,9				

With face grain in X -direction:

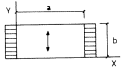
$$\alpha_{v1} = \alpha \sqrt[4]{\frac{E_{\perp}}{E_{//}}} = \alpha \sqrt[4]{\frac{500}{8000}} = 0,5\alpha$$

$$n = \frac{1/6 G t^3 \cdot 12(1 - \nu_x \nu_y)}{t^3 \sqrt{E_{//} E_{\perp}}} = \frac{2.750}{\sqrt{4000000}} = 0,75$$

With face grain in Y -direction:

$$\alpha_{v2} = \alpha \sqrt[4]{\frac{E_{//}}{E_{\perp}}} = \alpha \sqrt[4]{\frac{8000}{500}} = 2\alpha$$

Table 10. Calculated values of σ_{cr} and test results. Panels with clamped edges in X -direction, loaded \perp grain of face veneers



				α						
				1/2	1	1 1/2	2	2 1/2	3	
400	8	calculated	TGH	α_v	1	2	3	4	5	6
				σ_{cr}	4,85	4,37	4,48	4,37	4,39	4,48
		mea- surements	α_v	0,81	1,46	2,16	3,63			4,00
			σ_{cr}	8,25	9,56	9,29	7,37			8,68
		test	σ_{cr}	6,60	6,53	5,45	3,7			7,60
			σ_{ult}	8,74	11,1	11,4	6,58			11,9
	13	calculated	TGH	α_v	0,67	1,34	2,01	2,68	3,35	4,02
				σ_{cr}	21,5	21,5	21,5	21,5	21,5	21,5
		mea- surements	α_v	0,74	1,40	5,60	2,23			3,59
			σ_{cr}	18,3	20,3	33,5	27,8			30,5
		test	σ_{cr}	12,0	8,58	11,6	11,8			11,0
			σ_{ult}	13,4	13,8	19,4	16,3			14,8
600	8	calculated	TGH	α_v	1	2	3	4		
				σ_{cr}	1,68	1,47	1,57	1,58		
		mea- surements	α_v	0,71	1,68	2,22	2,75			
			σ_{cr}	3,03	3,51	3,53	4,20			
		test	σ_{cr}	2,32	2,12	2,35	2,49			
			σ_{ult}	5,68	5,69	7,32	7,35			
	13	calculated	TGH	α_v	0,67	1,34	2,01	2,68		
				σ_{cr}	8,27	8,27	8,27	8,27		
		mea- surements	α_v	0,64	1,58	1,61	2,23			
			σ_{cr}	7,75	14,4	10,3	9,86			
		test	σ_{cr}	6,86	7,40	5,26	5,23			
			σ_{ult}	9,30	9,79	10,1	9,58			

For 13 mm plywood $E_{//} = 8000 \text{ N/mm}^2$

$$E_{\perp} = 2500 \text{ N/mm}^2$$

$$G = 750 \text{ N/mm}^2$$

Now

$$\alpha_{v1} = \alpha \sqrt[4]{\frac{2500}{8000}} = 0,75\alpha$$

$$n = \frac{2 \times 0,75}{\sqrt{20 \cdot 10^6}} = 0,36$$

$$\alpha_{v2} = \alpha \sqrt[4]{\frac{8000}{2500}} = 1,34\alpha$$

With these values of E , G , α_{vs} , and η the practical design values of σ_{cr} were calculated. These should be a safe approximation of the actual values of σ_{cr} .

The 3rd and 4th line in the tables give calculated values of σ_{cr} , according to measurements; in this case values of σ_{cr} are based upon the measured values of N_x , N_y and N_{xy} of each panel separately. If the theory is valid for plywood and if in our test set-up the boundary conditions are not too inaccurate, these calculated values of σ_{cr} should be in good agreement with the actual test values. These actual values are listed in the 5th and 6th lines of the table; here σ_{cr} is the critical value determined from the deflections as shown in Fig. 8; σ_{ult} is the mean stress reached at the maximum load (post-buckling strength).

For the simply-supported panels, Figs. 11 to 18 give also the different values. From these diagrams it is evident that the design values of the TGH lead to conservative values of σ_{cr} ; they are on the safe side. The mean value of the ratio

$$\frac{\sigma_{cr, \text{test}}}{\sigma_{cr, \text{TGH}}} = 1,48,$$

with a standard deviation of 0,58; the smallest ratio in the tests was 0,84, the greatest 3,21. In Fig. 19 values of $\sigma_{cr, \text{test}}$ and $\sigma_{cr, \text{TGH}}$ are plotted; corresponding values must be expected to lie above the straight 45°-line; only three results show lower values.

The ratio

$$\frac{\sigma_{cr, \text{test}}}{\sigma_{cr, \text{calc. meas.}}}$$

can be used to check if the theory holds for the plywood panels. The calculated values of σ_{cr} are in this case based on the measured quantities N_x , N_y and N_{xy} . The mean value of the ratio

$$\frac{\sigma_{cr, \text{test}}}{\sigma_{cr, \text{calc. meas.}}} = 1,13,$$

with a standard deviation of 0,32; the smallest ratio was 0,68, the largest 2,10. In Fig. 20 values of $\sigma_{cr, \text{test}}$ and $\sigma_{cr, \text{calc. meas.}}$ are plotted; corresponding values should lie on the straight 45°-line.

Deviations of the expected and the test values may be ascribed to friction in the supports along the edges as described before.

For the plates with clamped edges it appears that the test results are essentially lower than the calculated values. Also from the deformations it becomes clear that the supposed cosine line between the clamped edges does not occur but that something much more like a sine line is obtained. This means that even the rather heavy clamping pressure along the steel clamping blocks is not enough to realise this theoretical situation. It must therefore be doubted whether in practice such clamped edges can indeed be

σ_{cr} and σ_{ult} for simply-supported panels, loaded // grain of face veneers ;
 $b = 400 \text{ mm}$; $t = 8 \text{ mm}$.

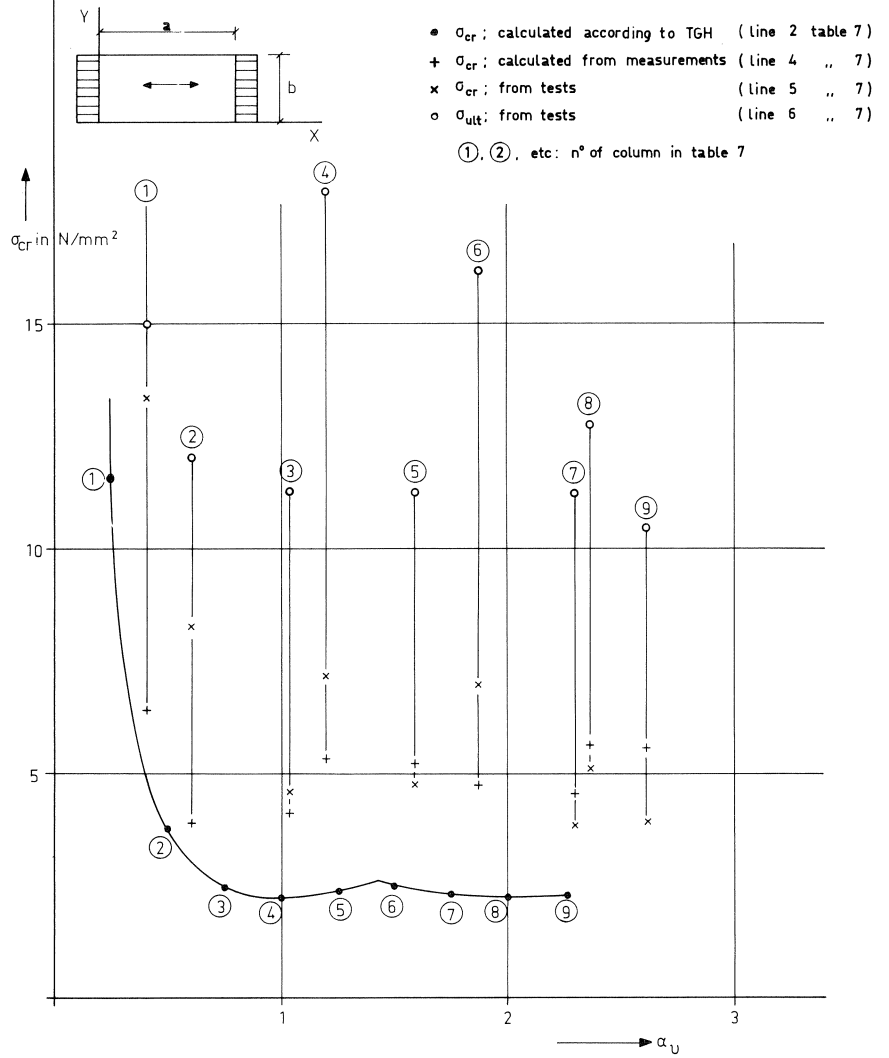


Fig. 11.

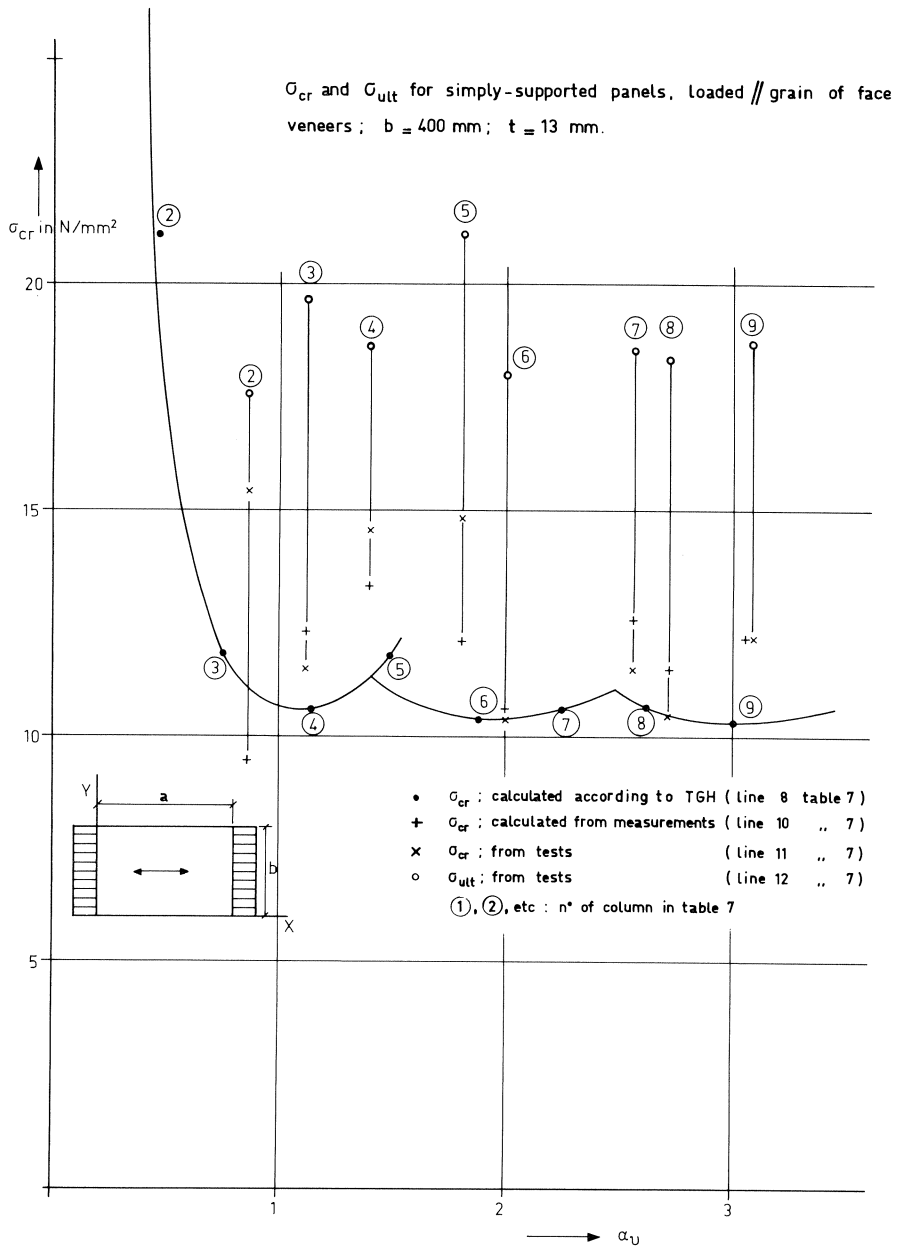


Fig. 12.

σ_{cr} and σ_{ult} for simply-supported panels, loaded // grain of face veneers,
 $b = 600$ mm, $t = 8$ mm.

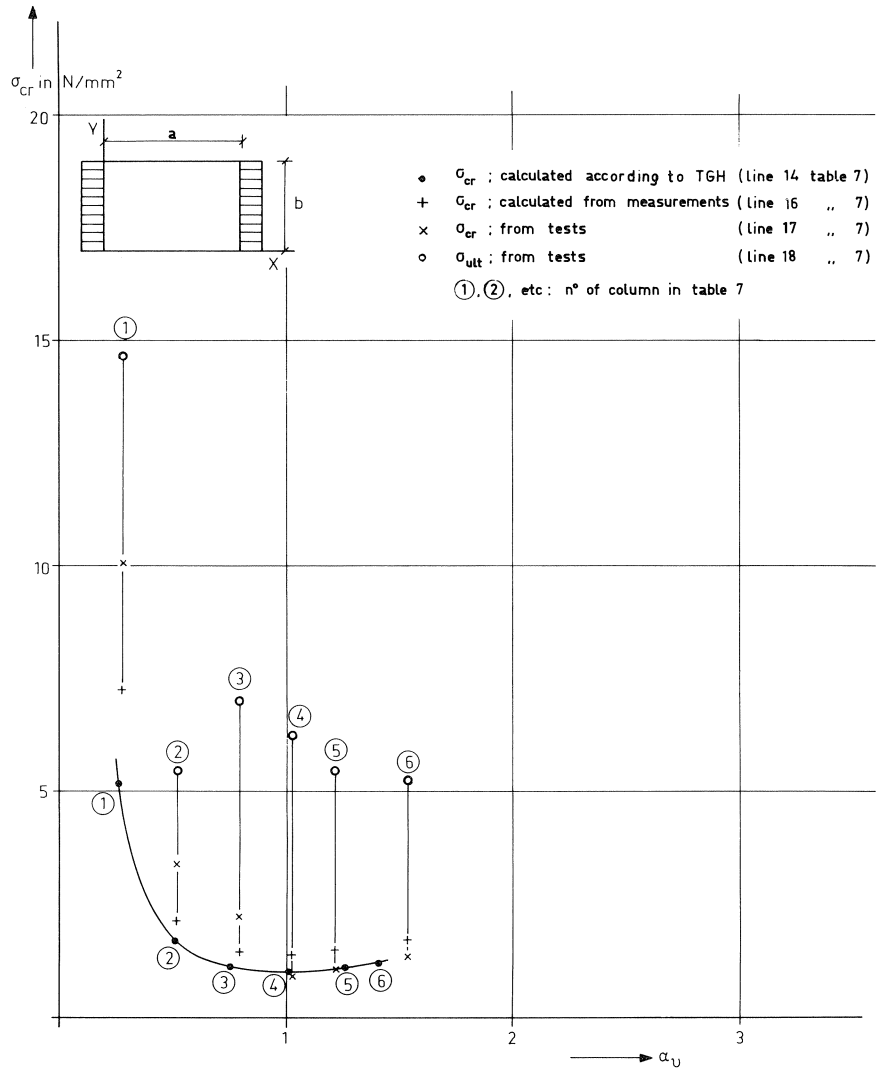


Fig. 13.

σ_{cr} and σ_{ult} for simply-supported panels, loaded // grain of face veneers ;
 $b = 600 \text{ mm}$, $t = 13 \text{ mm}$

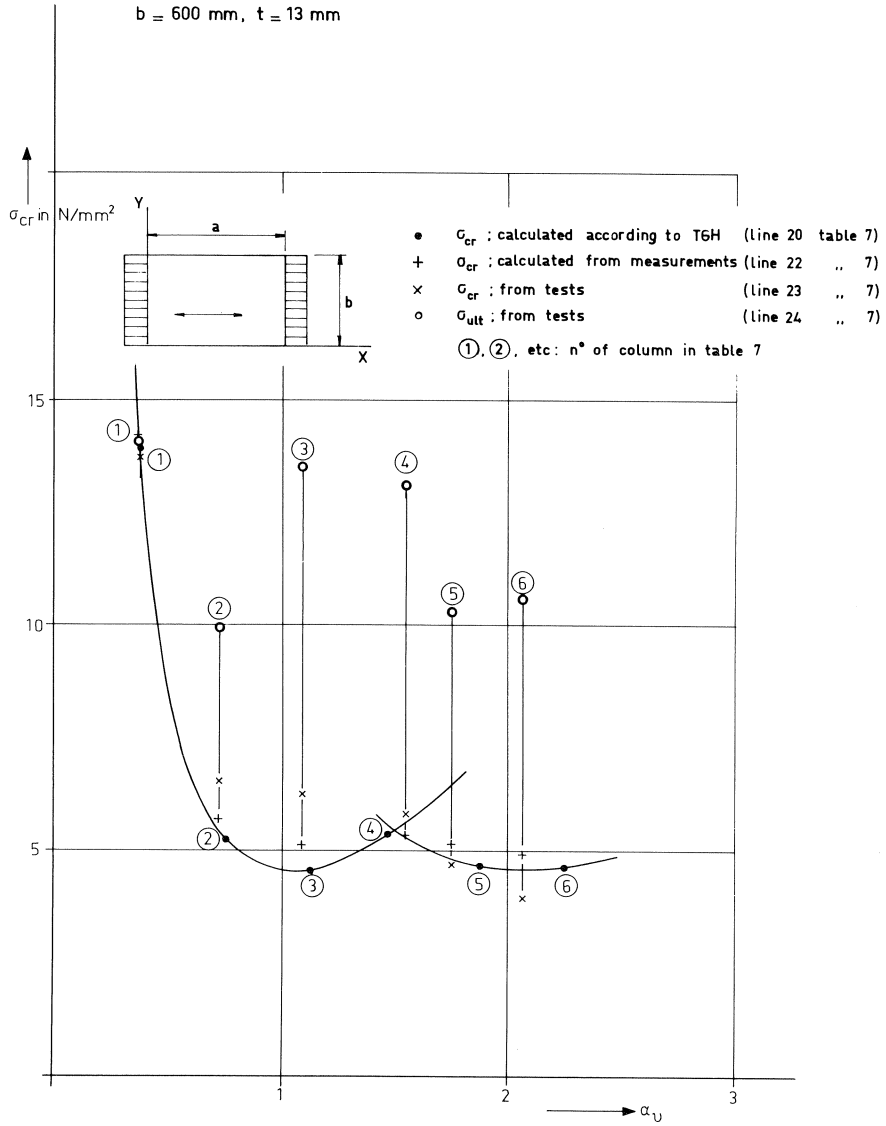
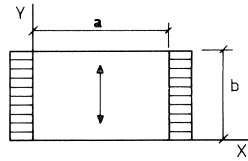


Fig. 14.

σ_{cr} and σ_{ult} for simply-supported panels, loaded \perp grain of face veneers; $b = 400\text{ mm}$ $t = 8\text{ mm}$



- σ_{cr} : calculated according to TGH (line 2 table 8)
 - + σ_{cr} : calculated from measurements (line 4 .. 8)
 - x σ_{cr} : from tests (line 5 .. 8)
 - o σ_{ult} : from tests (line 6 .. 8)
- ①, ②, etc : n° of column in table 8.

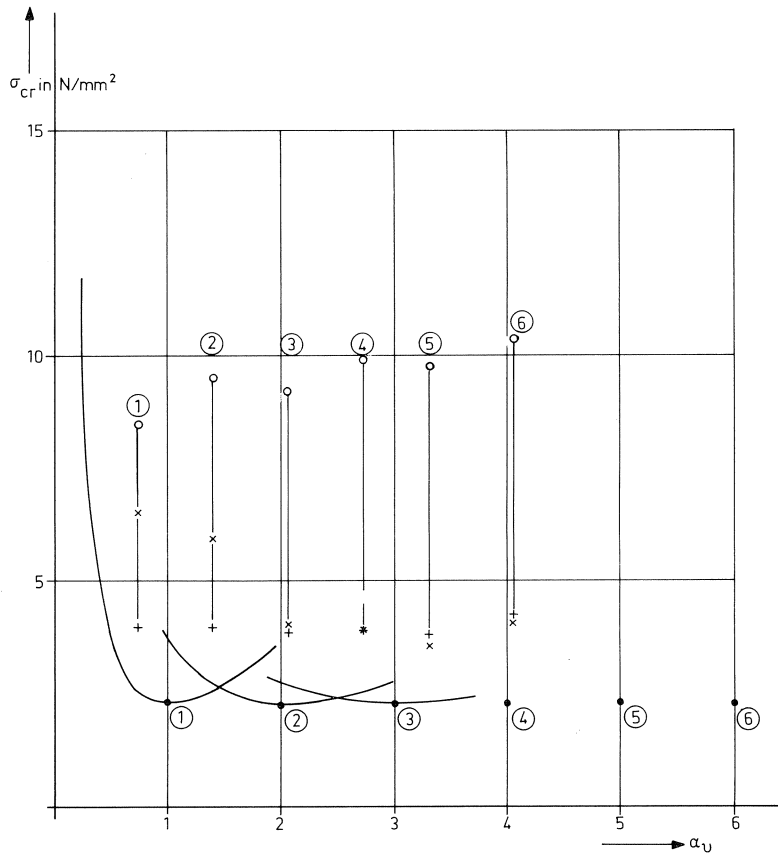


Fig. 15.

G_{cr} and G_{ult} for simply-supported panels, loaded \perp grain of face veneers; $b = 400$ mm, $t = 13$ mm

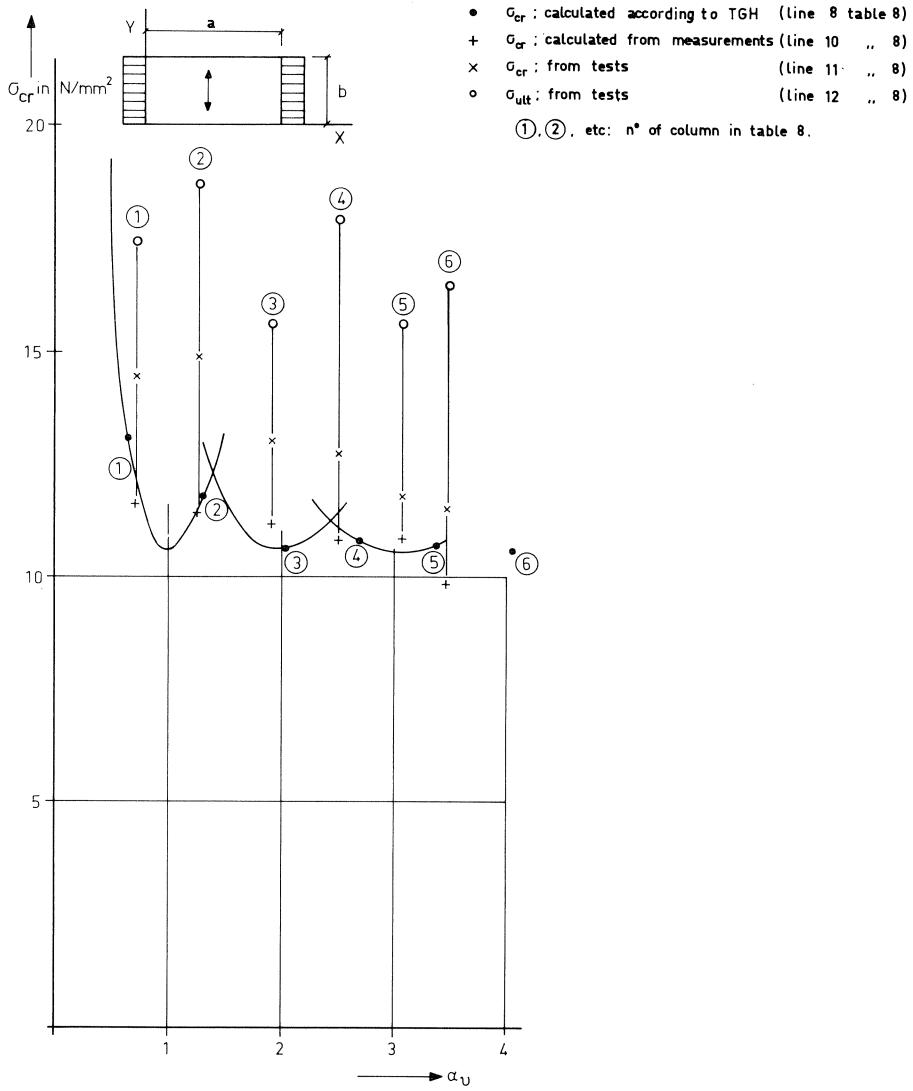


Fig. 16.

σ_{cr} and σ_{ult} for simply-supported panels, loaded \perp grain of face veneers ; $b=600$ mm ; $t=8$ mm

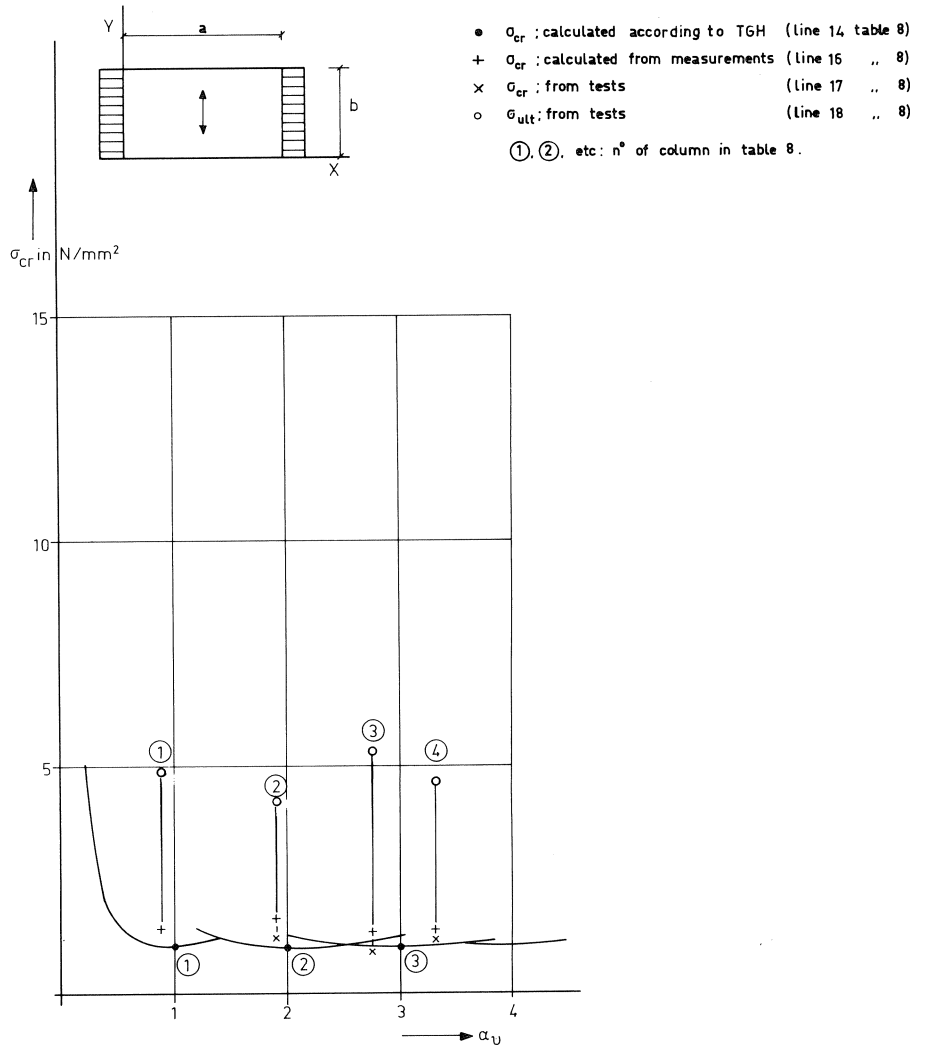
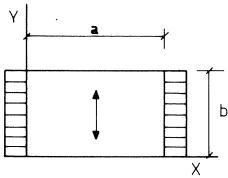


Fig. 17.

σ_{cr} and σ_{ult} for simply-supported panels, loaded \perp grain of face veneers; $b = 600$ mm, $t = 13$ mm



- σ_{cr} ; calculated according to TGH (line 20 table 8)
 - + σ_{cr} ; calculated from measurements (line 22 .. 8)
 - × σ_{cr} ; from tests (line 23 .. 8)
 - σ_{ult} ; from tests (line 24 .. 8)
- ①, ②, etc: n° of column in table 8.

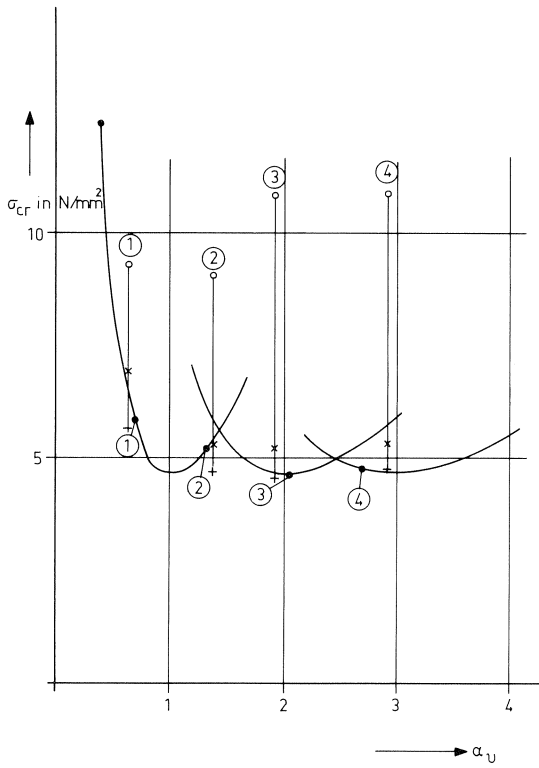


Fig. 18.

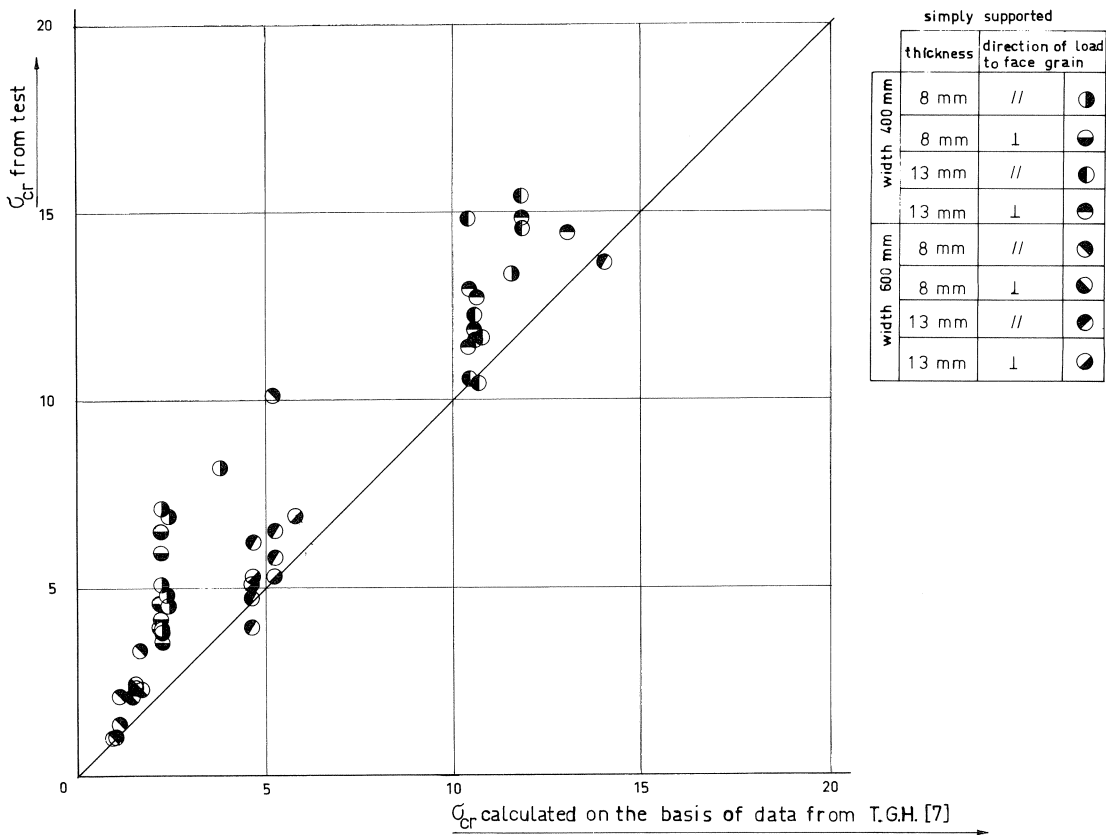


Fig. 19.

achieved. In most cases the critical stresses as well as the ultimate stresses are somewhat higher for the clamped panels than for the simply-supported ones.

4 Conclusions

There is good agreement between the test results σ_{cr} and the theoretical values calculated on the basis of measured dimensions and properties of the panels, This holds for the simply-supported panels.

Deviations must partly be ascribed to friction along the edges of the panels. The panels with clamped edges did not reach the expected values, most probably due to insufficient clamping. It must therefore be doubted whether in practice effective clamping can be achieved.

The values of σ_{cr} calculated on the basis of design values in the TGH are much on the safe side.

Safety is furthermore increased by the fact that the post-buckling strength is generally much higher than σ_{cr} . Only in very short panels did this effect disappear; in those cases the compressive strength of the plywood determined the strength.

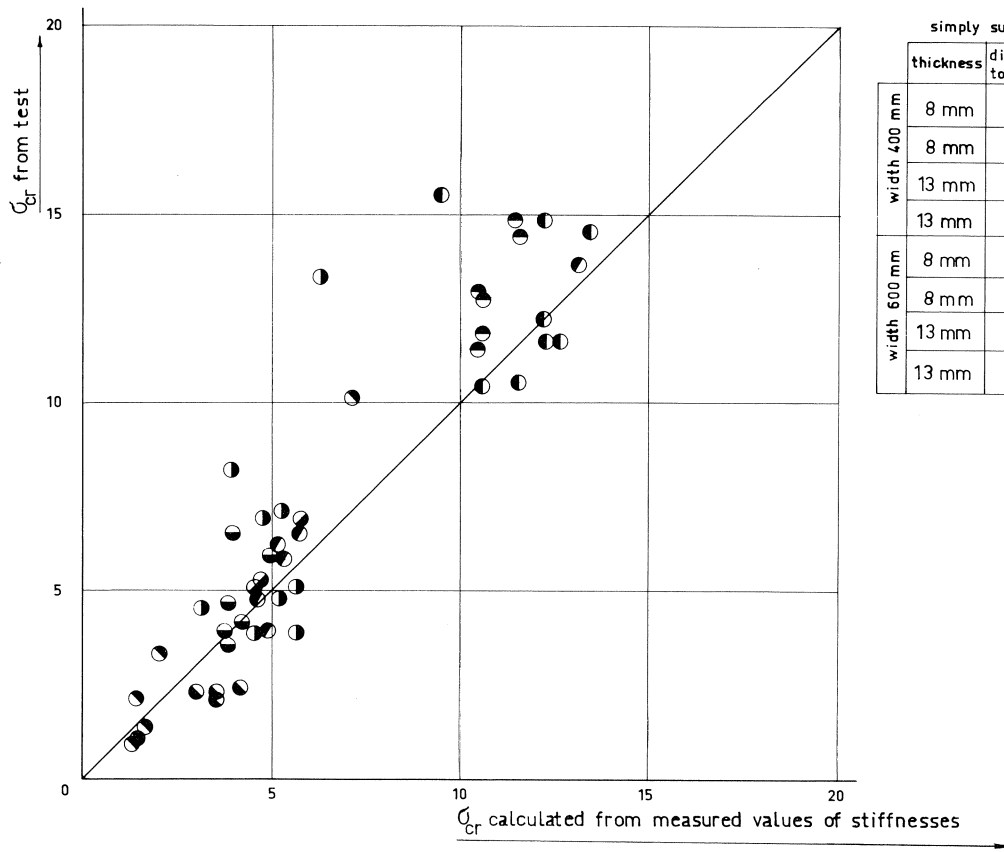


Fig. 20.



Fig. 21.

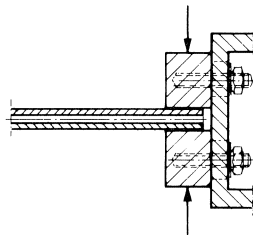


Fig. 22.

5 Recommendations for design

Assuming, on the basis of the foregoing, that the theories developed by several authors are a good tool for the prediction of the behaviour of plywood, the theory has been elaborated for more complex situations. These theoretical results lead to some design rules after simplifications have been made.

5.1 Theoretical values for various loading conditions

In the following it is assumed that a plywood plate can be loaded with normal and with shear stresses along the edges. The theory is limited to combinations of normal stresses which are linearly distributed and shear stresses which are uniform along the edges. Both cases will be dealt with separately and afterwards combinations will be studied.

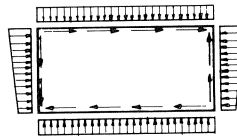


Fig. 23.

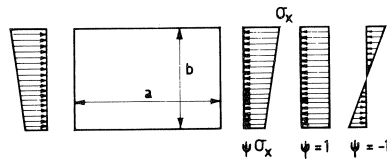


Fig. 24.

5.1.1 Normal stresses

For the orthotropic material it can be shown that the critical stress σ_{xcr} can be calculated following

$$\sigma_{xcr} = K \frac{4\pi^2}{b^2 t} \sqrt{N_x N_y}$$

where (cf. Fig. 24):

- σ_x = highest value of the compressive stress
- $\Psi \cdot \sigma_x$ = the other normal stress
- σ_{xcr} and $\Psi \sigma_{xcr}$ = the critical values of σ_x and $\Psi \sigma_x$
- N_x and N_y = plate stiffness as defined before
- K = buckling factor, the values of which depends on

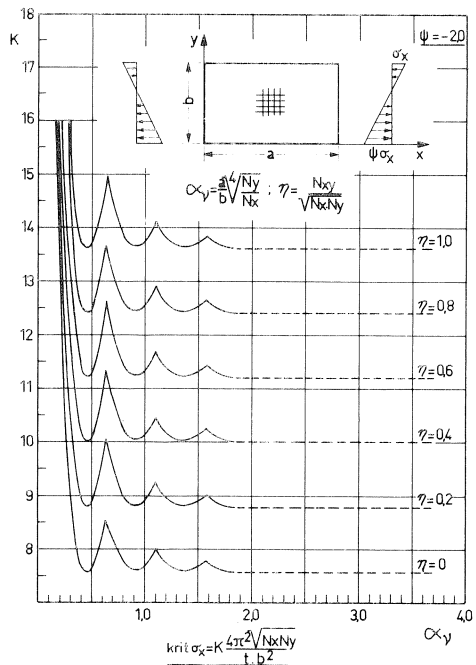
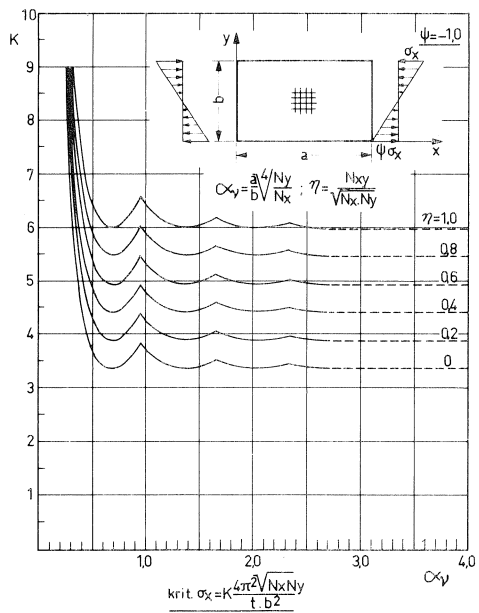
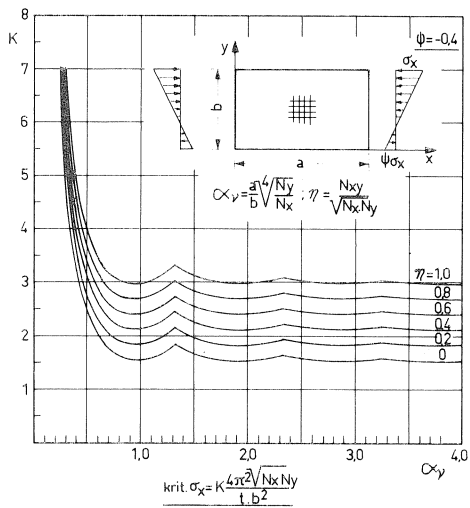
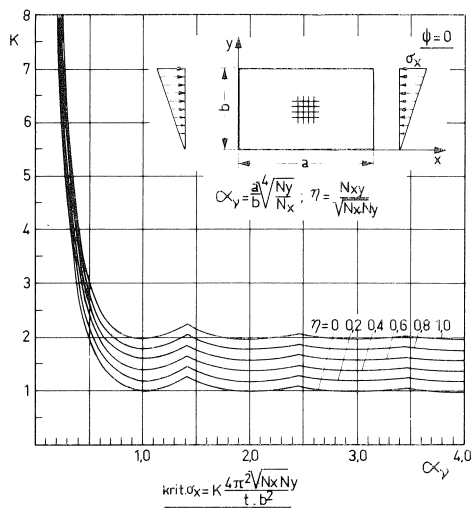
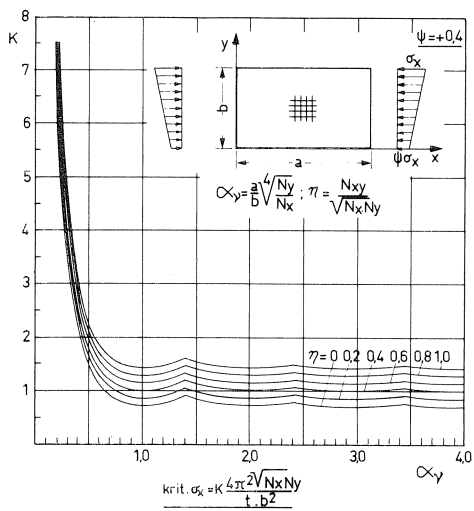
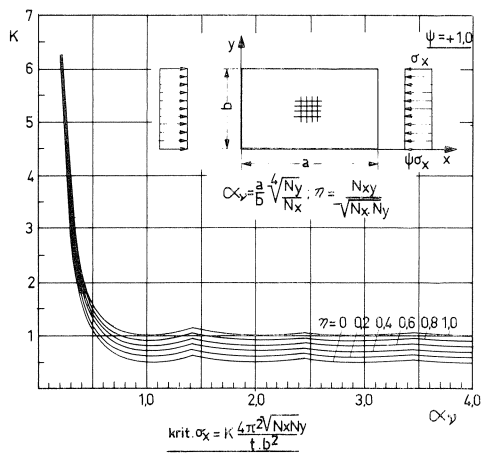


Fig. 25.

$$\alpha_v = \alpha \sqrt[4]{\frac{N_y}{N_x}} \text{ as well as on } \psi \text{ and on } \eta = \frac{N_{xy}}{\sqrt{N_x N_y}}$$

“Festoon” curves for different values of ψ and dependent on α are given in Fig. 25. It appears that ψ and η both have great influence. For constant values of ψ and η the effect of α_v is less important if $\alpha_v \gg 1$; at least for design purposes it seems to be justified to neglect this effect. This means that then the effect of $\alpha = a/b$ and of the number of half waves no longer plays any part. This leads to a graph as given in Fig. 26, where the minimum values of the curves of Fig. 25 are adopted as sufficiently accurate values for K .

If, as in [3] $v_x = v_y = 0$, then

$$N_x = \frac{E_x t^3}{12}, \quad N_y = \frac{E_y t^3}{12}, \quad N_{xy} = \frac{E_{xy} t^3}{6}, \quad \text{and} \quad \eta = \frac{2E_{xy}}{\sqrt{E_x E_y}}$$

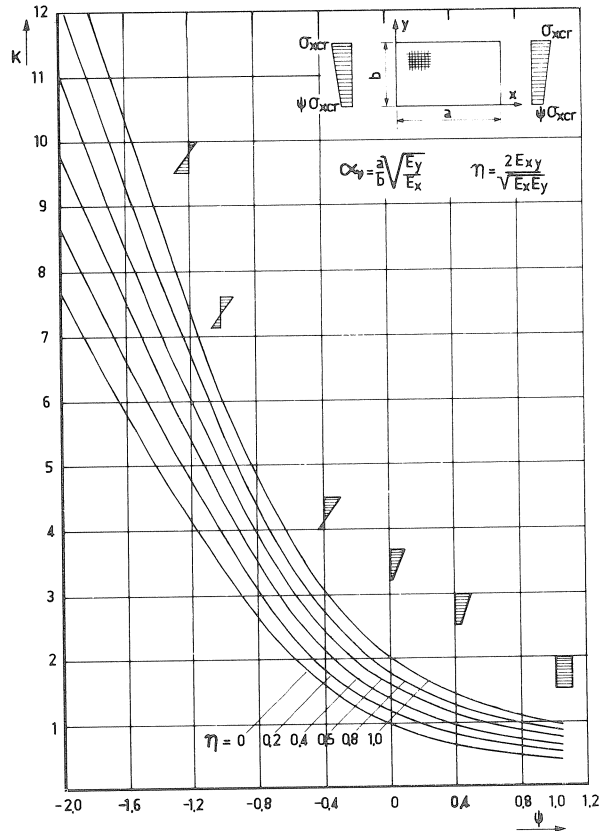


Fig. 26. Practical approximation of buckling factor K for simply-supported plates, loaded with linearly distributed normal stresses σ_x .

with which

$$\sigma_{cr} = K \cdot \frac{\pi^2 t^2}{3b^2} \sqrt{E_x E_y}.$$

Further simplification can be achieved, if for a certain material or a group of materials the value of γ_j deviates not too much from a mean value. In that case K could be given, for example, for the most frequent compression load ($\Psi = 1$) and for bending ($\Psi = -1$); together with some realistic values of E_x and E_y really simple design formulas can be found.

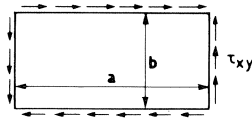


Fig. 27.

5.1.2 Shear stresses

The relatively simple case of constant shear stress τ along the edges is considered here. According to [3] it can be shown that

$$\tau_{cr} = K \frac{4\pi^2}{b^2 t} \sqrt{N_x N_y^3}$$

With $\nu_x = \nu_y = 0$ this becomes

$$\tau_{cr} = K \cdot \frac{\pi^2 t^2}{3b^2} \sqrt{E_x E_y^3}$$

Values of K can be read from Fig. 28, which graph can for practical purposes be simplified to Fig. 29, where the “wrinkles” of the curves – depending on the number of half-waves – are neglected and where for practical reasons a tangent is used for $\alpha_v < 1$ instead of the asymptotic curves.

Because of the variability in the thickness and mechanical properties of plywood t is not possible to arrive at an accurate value of α_v . The original Fig. 28 gives way to very different values of K with small changes of α_v if $\alpha < 1$; this effect has been avoided with the use of the tangents instead of the curves.

5.1.3 Combinations of bending or normal stresses with shear

If the symbols σ_{xcr} and τ_{cr} used also for the plate with normal and shear stress only, and if σ_{crx}^1 and τ_{cr}^1 are used for normal and shear stresses in combination, according to [3],

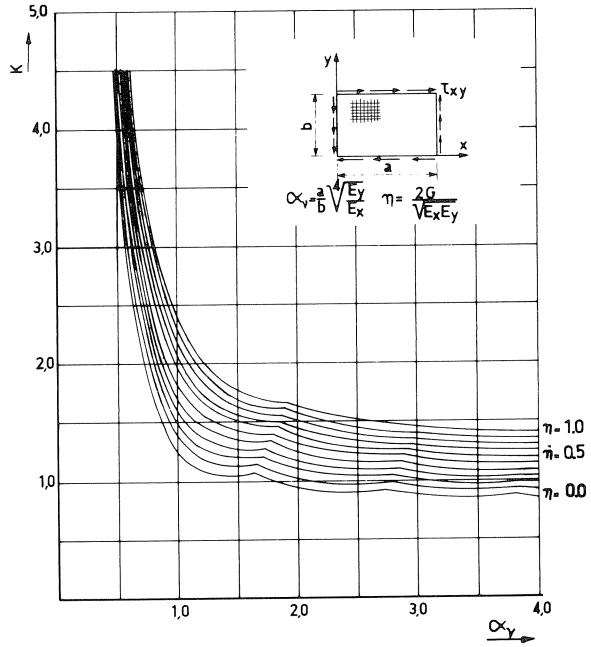


Fig. 28. Buckling factor K for simply-supported plates loaded with constant shear stresses τ_{xy} [3].

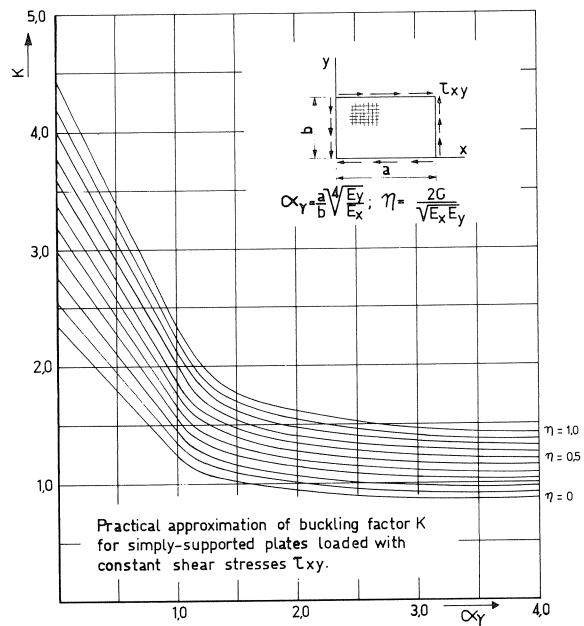


Fig. 29. Practical approximation of buckling factor K for simply-supported plates loaded with constant shear stresses τ_{xy} .

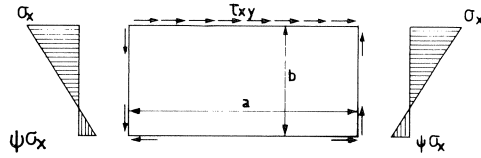


Fig. 30.

graphs can be plotted in which the relationship between $\sigma_{crx}^1/\sigma_{crx}$ and τ_{cr}^1/τ_{cr} is given both for the case where $\Psi = 1$ and $\Psi = -1$ (cf. Fig. 31).

The curves in Fig. 31a are partly more or less parabolic; in Fig. 31b the circle is a better approximation. For reasons of simplicity it is proposed to use a safe circular boundary

$$\left(\frac{\sigma_{crx}^1}{\sigma_{crx}}\right)^2 + \left(\frac{\tau_{cr}^1}{\tau_{cr}}\right)^2 = 0,85 (= 0,92^2)$$

This circle is also given in Fig. 31.

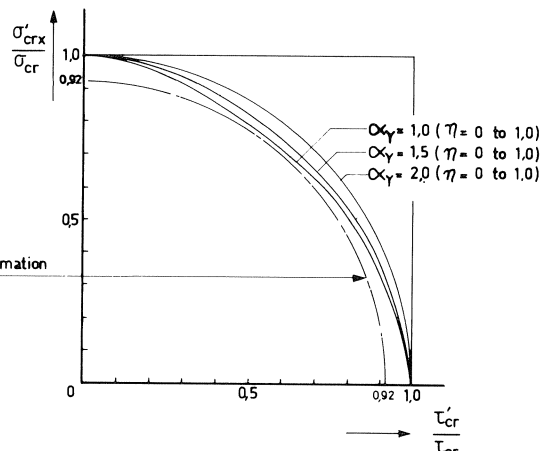
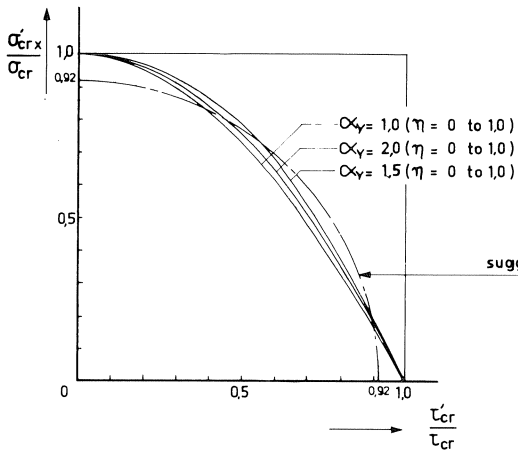
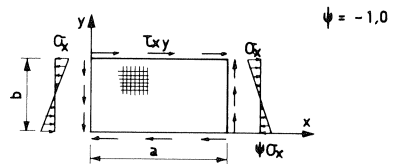
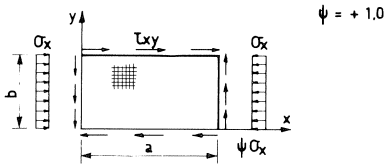


Fig. 31. Approximation of calculation boundary for stress combinations by a circle.

5.1.4 Combination of normal stress in two directions (uniformly distributed)

If again σ_{crx}^1 and σ_{cry}^1 are used as the symbols for the combined actions and if σ_{crx} and σ_{cry} are the critical values where there are only stress in the X- or in the Y-direction, it can be shown that the following relationship holds (see Appendix):

$$\frac{\sigma_{crx}^1}{\sigma_{crx}} + \frac{\sigma_{cry}^1}{\sigma_{cry}} = 1$$

which is a straight line in Fig. 33.

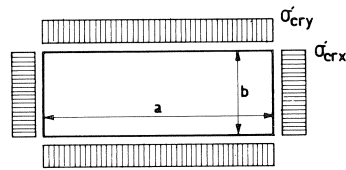


Fig. 32.

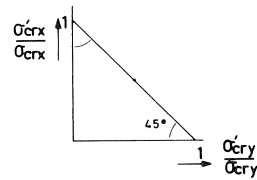


Fig. 33.

5.1.5 Combination of two normal and shear stresses

Based upon the relationships in the foregoing it seems not too risky to extend the boundaries to a three-dimensional system such as Fig. 34, which could be described by

$$\left(\frac{\sigma_{crx}^1}{\sigma_{crx}} + \frac{\sigma_{cry}^1}{\sigma_{cry}}\right)^2 + \left(\frac{I_{cr}^1}{I_{cr}}\right)^2 = 0,85$$

This three-dimensional diagram is only an extrapolation of the three boundaries in the three main planes; there is no verification available as yet.

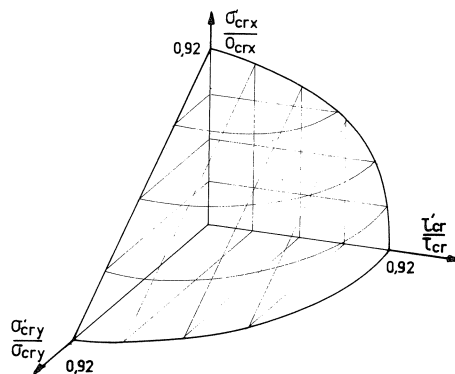


Fig. 34.

6 Aspects of safety

Assuming that the design values of the TGH will remain unchanged, design calculations will be based on them in the near future. Safe design values for buckling must therefore also be based upon the TGH.

In Tables 7 and 8 values have been given for $\sigma_{cr;TGH}$ and $\sigma_{cr;test}$. For the simply-supported panels - the clamped panels are not considered here any more - the mean value of the ratio $\sigma_{cr;test}/\sigma_{cr;TGH}$ was 1,48, with a standard deviation of 0,58.

In Table 11 the values are given in certain groups, from which a coefficient of variation can be calculated, according to

$$v_{\text{mean}} = \sqrt{\frac{\sum[(n_i - 1)v^2]}{\sum(n_i - 1)}}$$

from which $v_{\text{mean}} = 0,19$.

Table 11. Values of $\sigma_{cr;test}/\sigma_{cr;TGH}$; simply-supported panels

<i>b</i>	<i>t</i>	// or ⊥	ratio	st.dev.	var. coeff.	<i>n</i>
400	8	//	1,99	0,25	0,12	9
	13	//	1,16	0,15	0,13	8
	8	⊥	2,16	0,54	0,25	6
	13	⊥	1,18	0,07	0,06	6
600	8	//	1,49	0,53	0,35	6
	13	//	1,09	0,18	0,17	6
	8	⊥	1,04	0,15	0,15	3
	13	⊥	1,08	0,09	0,08	4

This latter estimate is a better one than the one calculated earlier, because here the systematic errors for the various groups are eliminated. Using this coefficient of variation, an allowable value of a buckling stress can be calculated according to the theory in [6], from which

$$\bar{\sigma}_{cr} = \frac{\sigma_{cr;TGH}}{2,1}$$

where no reduction for long time loading is as yet introduced. With respect to the test values there is a mean safety of $\approx 3,1$

$$\left(\bar{\sigma}_{cr} = \frac{1,48 \cdot \sigma_{cr;TGH}}{2,1 \times 1,48} = \frac{\sigma_{cr;test}}{3,11} \right)$$

It is assumed furthermore that a good approximation of the behaviour of the plywood plate under increasing loads, after creep and possible other effects have taken place, is

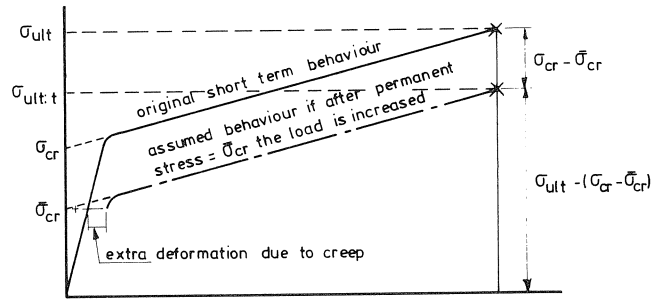


Fig. 35.

given by the - - line in Fig. 35. From this diagram it is clearly assumed that, after the creep period at full σ_{cr} , an overload causes deformations on the basis of the original plate stiffness. Failure is assumed to occur at the same deformation as in the short-duration test. As $\sigma_{ult} \approx 2\tau_{cr}$ failure after constant preload to $\bar{\sigma}_{cr}$ occurs at a load of

$$\begin{aligned} \sigma_{ult} - (\sigma_{cr} - \bar{\sigma}_{cr}) &= 2\sigma_{cr} - (\sigma_{cr} - 0,32\sigma_{cr}) \\ &= 1,32\sigma_{cr}, \text{ i.e., at } \frac{1,32\sigma_{cr}}{0,32\sigma_{cr}} \approx 4 \times \bar{\sigma}_{cr} \end{aligned}$$

On the basis of the foregoing a set of limits to the stresses can be proposed:

1. the calculated stresses in a plate, resulting from the loads on the structure, must not exceed the allowable normal stress $\bar{\sigma}_{comp}$ and the allowable shear stress $\bar{\tau}$
2. the calculated stresses must not exceed allowable critical stresses $\bar{\sigma}_{cr}$, $\bar{\tau}_{cr}$ or certain combinations thereof.

In the case of stress combinations the calculated stresses σ_x , τ_y and τ must satisfy the equation:

$$\left(\frac{\sigma_x}{\bar{\sigma}_{xcr}} + \frac{\sigma_y}{\bar{\sigma}_{ycr}} \right)^2 + \left(\frac{\tau}{\bar{\tau}_{cr}} \right)^2 \leq 0,85$$

For practical purposes the following equation can be used:

$$\left(\frac{\sigma_x}{\bar{\sigma}_{xcr}} + \frac{\sigma_y}{\bar{\sigma}_{ycr}} \right)^2 + \left(\frac{\tau}{\bar{\tau}_{cr}} \right)^2 \leq 1$$

In this case we have to multiply the formulae for $\bar{\sigma}_{xcr}$, $\bar{\sigma}_{ycr}$ and $\bar{\tau}_{cr}$ by a factor 0,92.

Based on the foregoing, the behaviour of plywood as a structural material in load bearing structures can be analysed. For practical purposes, sets of calculated values for various plywood and for certain loading conditions can be given. Experience and further research may lead to the adoption of lower safety factors in the future.

References

1. TIMOSHENKO and GERE, Theory of elastic stability, McGraw-Hill Book Comp. Inc.
2. LEKNITSKII, S. G., Anisotropic Plates, Gordon and Breach Science Publishers.
3. HALASZ, R. VON und E. CZIESIELSKI, Berechnung und Konstruktion geleimter Träger mit Stegen aus Furnierplatten, Berichte aus der Bauforschung, Heft 47, Wilhelm Ernst & Sohn.
4. DEKKER, J. N., Plooigedrag van Canadees Oregon pine triplex // en \perp de vezelrichting van de dekfineerlaag, Rapport 4-73-16-T13, Stevinlaboratorium Delft.
5. PLOOS VAN AMSTEL, H., De berekening van het instabiliteitsgedrag van triplex in constructies; voorstellen voor richtlijnen, Rapport 4-75-1, TC 34, Stevinlaboratorium Delft.
6. KUIPERS, J., Structural Safety, Heron; English edition No. 5 (1968), Delft.
7. Anon. Tabellen en Grafieken voor Houtconstr. TGH publ. Houtvoorlichtingsinst. HVI Amsterdam.

APPENDIX I

Stability of a rectangular orthotropic plate compressed in two directions

A rectangular plate of thickness t and with its principal directions parallel to the edges is compressed by uniformly distributed stresses σ_x and σ_y . The problem of stability of such a plate has been solved for the case of four supported edges (see Lekhnitskii: "Anisotropic plates"). The differential equation will have the form:

$$N_x \frac{\partial^4 w}{\partial x^4} + 2N_{xy} \frac{\partial^4 w}{\partial x^2 \partial y^2} + N_y \frac{\partial^4 w}{\partial y^4} + t\sigma_x \frac{\partial^2 w}{\partial x^2} + t\sigma_y \frac{\partial^2 w}{\partial y^2} = 0 \quad (1)$$

For a solution in the form of:

$$w = \sum_m \sum_n A_{mn} \sin \frac{m\pi x}{a} \sin \frac{n\pi y}{b}$$

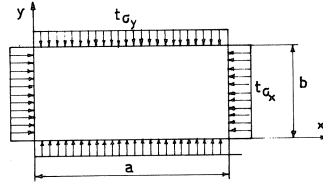


Fig. 1. Rectangular plate compressed in two directions.

We obtain the relation:

$$t\sigma_x \left(\frac{m}{a}\right)^2 + t\sigma_y \left(\frac{n}{b}\right)^2 = \pi^2 \left[N_x \left(\frac{m}{a}\right)^4 + 2N_{xy} \left(\frac{mn}{ab}\right)^2 + N_y \left(\frac{n}{b}\right)^4 \right] \quad (2)$$

For the case where σ_x and σ_y vary but maintain a constant ratio:

$$\sigma_x = \zeta \quad \text{and} \quad \sigma_y = \varphi \zeta,$$

a critical value of ζ can be found as

$$\zeta_{cr} = \frac{\pi^2 \sqrt{N_x N_y}}{tb^2} \cdot \frac{\sqrt{\frac{N_x}{N_y} \left(\frac{m}{a}\right)^2} + \frac{2N_{xy}}{\sqrt{N_x N_y}} n^2 + \sqrt{\frac{N_y}{N_x} \left(\frac{a}{m}\right)^2} n^4}{1 + \varphi \left(\frac{a}{m}\right)^2 n^2}$$

$$= \frac{4\pi^2 \sqrt{N_x N_y}}{tb^2} \cdot \frac{\left(\frac{m}{2w\alpha}\right)^2 + 1/2\eta n^2 + \left(\frac{w\alpha}{2m}\right)^2}{1 + \varphi \left(\frac{\alpha}{m}\right)^2 n^2} \quad (3)$$

where:

- N_x, N_y = bending stiffness in x - and y -direction respectively
- N_{xy} = torsional stiffness
- t = thickness of the plate
- α = ratio a/b
- w = $\sqrt[4]{N_y/N_x}$
- n = $N_{xy}/\sqrt{N_x N_y}$
- m, n = number of waves in x - and y -direction respectively

From Lekhnitskii's formula 3 we can go further as follows: the critical value for ζ will be minimum when $n = 1$. Equation (3) reduces to:

$$\zeta_{cr} = \frac{4\pi^2 \sqrt{N_x N_y}}{tb^2} \cdot \frac{\left(\frac{m}{2w\alpha}\right)^2 + 1/2\eta + \left(\frac{w\alpha}{2m}\right)^2}{1 + \varphi \left(\frac{\alpha}{m}\right)^2} = \frac{\pi^2 \sqrt{N_x N_y}}{tb^2} \cdot K \quad (4)$$

For compression in the x -direction only: $\zeta_{cr| \varphi=0} = \sigma_{xcr}$; for compression in the y -direction only: $\varphi \zeta_{cr| \varphi=\infty} = \sigma_{y'cr}$. For other values of φ the combination:

$$\sigma'_{xcr} = \zeta_{cr} \quad \text{and} \quad \sigma'_{y'cr} = \varphi \zeta_{cr}$$

becomes critical.

In general we find the minimum value for ζ_{cr} by taking the minimum value of the second part of equation (4):

$$K = \frac{\left(\frac{m}{2w\alpha}\right)^2 + 1/2\eta + \left(\frac{w\alpha}{2m}\right)^2}{1 + \varphi \left(\frac{\alpha}{m}\right)^2} \quad (5)$$

In Fig. 2 the minimum values of K have been plotted for $w = 1$ and different values of $\eta = 1; \eta$ ($= 0; 0,2; 0,4; 0,6; 0,8; 1,0$) and φ ($= 0; 0,2; 1,0; 10,0$).

From equation (4) and for $m = 1$ we obtain the following relations:

$$\sigma'_{xcr} = \frac{\sigma_{xcr}}{1 + \varphi \alpha^2}; \quad \sigma'_{y'cr} = \frac{\varphi \sigma_{xcr}}{1 + \varphi \alpha^2} \quad \text{and} \quad \sigma'_{y'cr} = \frac{\sigma_{xcr}}{\alpha^2}$$

so that:

$$\frac{\sigma'_{xcr}}{\sigma_{xcr}} + \frac{\sigma'_{ycr}}{\sigma_{ycr}} = \frac{1}{1+\varphi\alpha^2} + \frac{\varphi\alpha^2}{1+\varphi\alpha^2} = 1 \quad (6)$$

From Fig. 2 it can be seen that for different values of φ and a particular value of α the minimum value of K will be reached for different values of m . In that case equation (6) does not hold anymore.

However, from Fig. 3 it can be seen that the differences from the straight line are rather small and that relation (6) is safe. These graphs are given for:

$$\begin{aligned} w &= 0,5; 1,0; 1,5; 2,0; \\ \eta &= 0,4; \\ \varphi &\text{ varies from 0 to 100.} \end{aligned}$$

However we want to use the real minimum value for K (see Fig. 2) so we have to check if relation (6) is also operative in that case. From $dK/d\alpha = 0$ (see equation 5) we obtain α where K is a minimum:

$$\alpha^2 = \varphi \frac{m^2}{w^2} \frac{1}{w^2 - 2\eta\varphi} \left[1 \pm \sqrt{1 + \frac{w^2}{\varphi^2} (w^2 - 2\eta\varphi)} \right]$$

Only for $w^2 - 2\eta\varphi > 0$ do we get real values for α and real minima for K . If $w^2 - 2\eta\varphi \leq 0$ the curve for K has no real minimum but an asymptote.

In case $w^2 - 2\eta\varphi > 0$ and for $\eta = 1$ we find:

$$\alpha^2 = \frac{m^2}{w^2 - 2\varphi}$$

so that:

$$K_{\min} = \left(1 - \frac{\varphi}{w^2} \right);$$

for $\eta = 0$ we find in case $\varphi \gg w^2$:

$$\alpha^2 = \frac{2m^2}{w^4} \varphi \quad \text{so} \quad K_{\min} = \frac{w^2}{4\varphi}$$

In case $\varphi \ll w^2$ we find:

$$\alpha^2 = \frac{m^2}{w^2} \quad \text{and} \quad K_{\min} = \frac{0,5}{1 + (\varphi/w^2)}$$

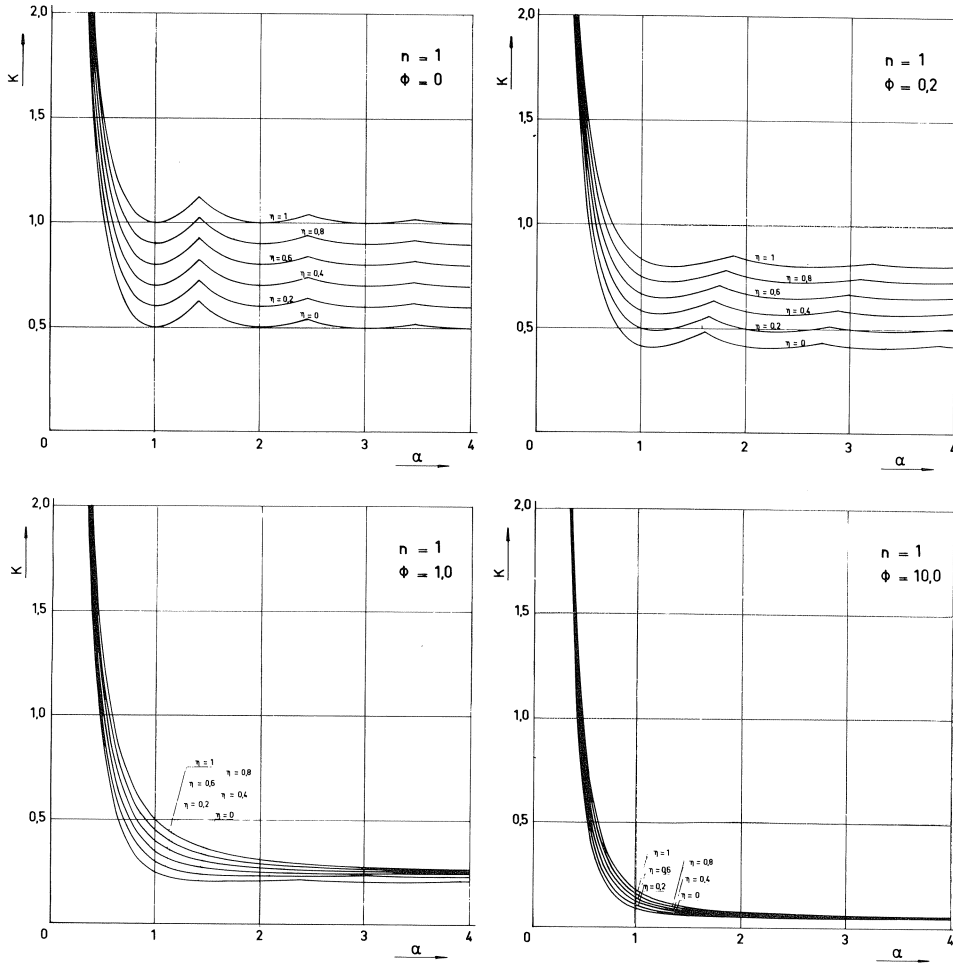


Fig. 2. Festoon curves for K for $w = E_y/E_x = 1$ and various values of η and ϕ .

Relation (6) becomes now:

$$\eta = 1: \frac{4(1-\phi/w^2)}{1} + \frac{4\phi(1-\phi/w^2)}{w^2} = 1 + \frac{3\phi}{w^2} - \frac{4\phi^2}{w^4}$$

The condition was $w^2 - 2\phi > 0$ or $\phi < 1/2w^2$. For $\phi = 0$ relation (5) becomes 1 and for $\phi \approx 1/2w^2$ relation (5) is less than 1,5.

$$\eta = 0 \text{ and } \phi \gg w^2: \frac{w^2/\phi}{2} + \frac{w^2}{w^2} = \frac{w^2}{2\phi} + 1 \approx 1$$

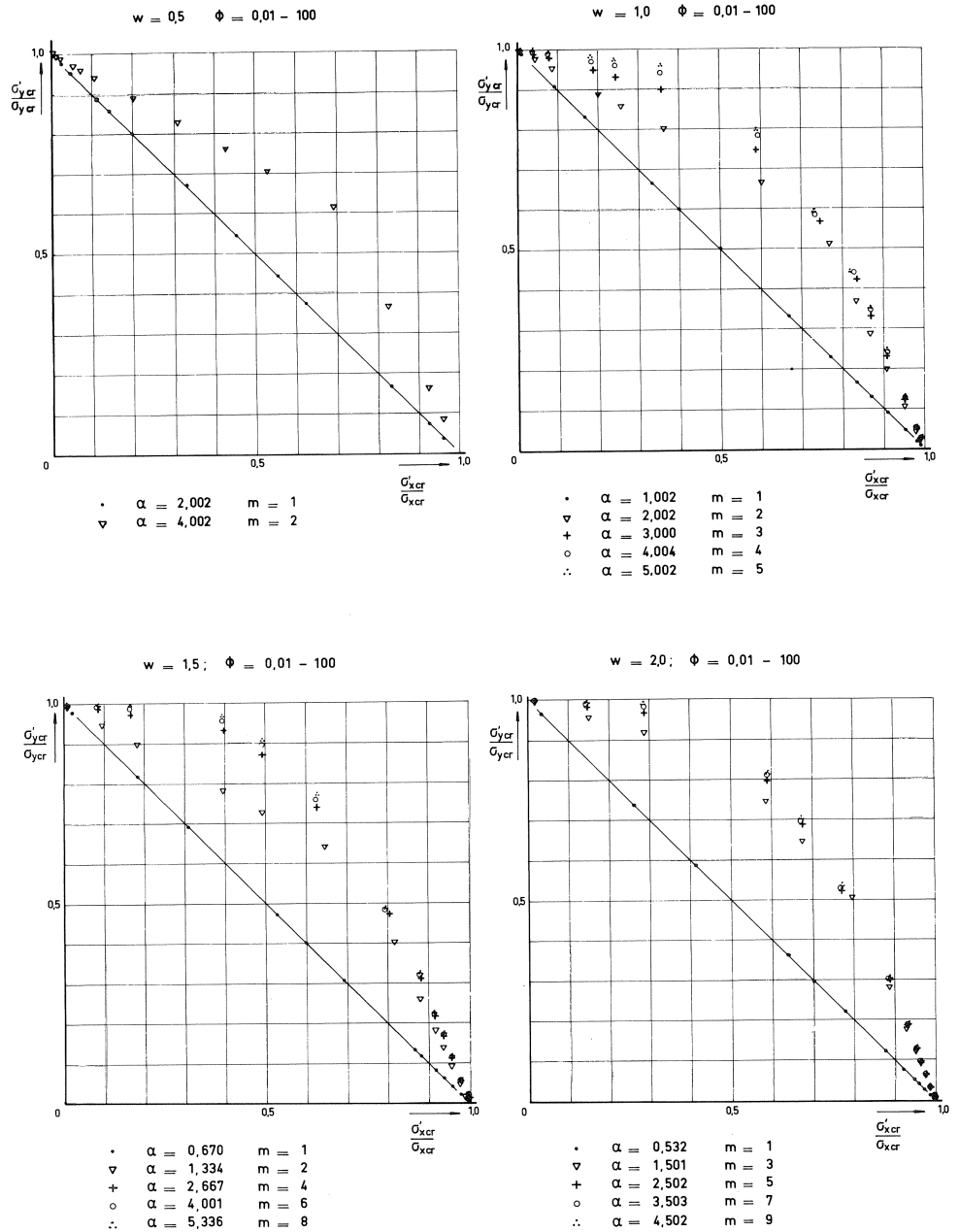


Fig. 3. Relation $\sigma'_{xcr}/\sigma_{xcr}$ and $\sigma'_{ycr}/\sigma_{ycr}$ for $\beta = 0$ and various values of α , w and ϕ .

$$\eta=0 \text{ and } \varphi \ll w^2: \frac{\frac{2}{1+\varphi/w^2} \varphi \cdot \frac{2}{1+\varphi/w^2}}{w^2} = \frac{w^2+2\varphi}{w^2+\varphi} \approx 1$$

As mentioned before, the curve K will have an asymptote when $w^2-2n\varphi \leq 0$. This asymptote is $K=w^2/\varphi$.

Relation (6) becomes now in the case $\eta=1(\varphi \geq 1/2w^2)$:

$$\frac{w^2/\varphi}{4} + \frac{w^2}{w^2} = 1 \text{ to } 1,125$$

and in the case $\eta > 0 (\varphi \rightarrow \infty)$ then relation (6) becomes equal to 1.

Both theoretically and based on the minimum values of K , relation (6) appears to be a rather good and safe relation to approximate the critical stability situation of a plate compressed in two directions. Relations (6) ranges between the values 1 and 1,5.

APPENDIX II

Stability of a rectangular orthotropic plate uniformly compressed in one direction and loaded by linearly distributed forces in the other direction

The problem of stability of an orthotropic plate loaded by linearly distributed forces in one direction has been solved by Lekhnitskii among others. The combination with uniformly distributed compression forces in the other direction (Fig. 4) can be solved as follows.

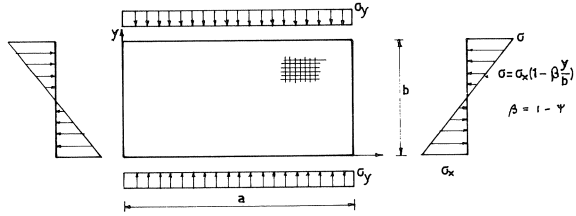


Fig. 4. Rectangular plate uniformly compressed in one direction and loaded by linearly distributed forces in the other direction.

The potential energy of the external loads is:

$$U = \int_0^a \int_0^b \frac{t\sigma_x}{2} \left(1 - \beta \frac{y}{b}\right) \left(\frac{dw}{dx}\right)^2 dx dy + \frac{t\sigma_y}{2} \int_0^a \int_0^b \left(\frac{\partial w}{\partial y}\right)^2 dx dy$$

The strain energy is:

$$I = 1/2 \int_0^a \int_0^b \left\{ N_x \left(\frac{\partial^2 w}{\partial x^2}\right)^2 + 2N_{xy} \left(\frac{\partial^2 w}{\partial x \partial y}\right)^2 + N_y \left(\frac{\partial^2 w}{\partial y^2}\right)^2 \right\} dx dy$$

The solution for the deflection that satisfies the boundary conditions is:

$$w = \sum_m \sum_n A_{mn} \sin \frac{m\pi x}{a} \sin \frac{n\pi y}{b}$$

When the number of waves in y -direction is fixed at $n = 2$, satisfactory accuracy can be expected to be attained. In that case the deflection is

$$w = \sum_m \left(A_{m1} \sin \frac{\pi y}{b} + A_{m2} \sin \frac{2\pi y}{b} \right) \sin \frac{m\pi x}{a}$$

This leads to:

$$\begin{aligned}\frac{\delta w}{\delta x} &= \left(A_{m1} \sin \frac{\pi y}{b} + A_{m2} \sin \frac{2\pi y}{b} \right) \cdot \frac{m\pi}{a} \cos \frac{m\pi x}{a} \\ \frac{\delta^2 w}{\delta x^2} &= - \left(A_{m1} \sin \frac{\pi y}{b} + A_{m2} \sin \frac{2\pi y}{b} \right) \cdot \left(\frac{m\pi}{a} \right)^2 \sin \frac{m\pi x}{a} \\ \frac{\delta^2 w}{\delta x \delta y} &= \frac{m\pi^2}{ab} \left(A_{m1} \cos \frac{\pi y}{b} + A_{m2} \cos \frac{2\pi y}{b} \right) \cos \frac{m\pi x}{a} \\ \frac{\delta^2 w}{\delta y^2} &= \frac{\pi^2}{b^2} \left(A_{m1} \sin \frac{\pi y}{b} + 2A_{m2} \sin \frac{\pi y}{b} \right) \sin \frac{m\pi x}{a}\end{aligned}$$

Substitution into the equation for the potential energy gives:

$$\begin{aligned}U &= \frac{t\sigma_x}{2} \int_0^a \int_0^b \left(1 - \beta \frac{y}{b} \right) \left(A_{m1} \sin \frac{\pi y}{b} + A_{m2} \sin \frac{2\pi y}{b} \right)^2 \left(\frac{m\pi}{a} \cos \frac{m\pi x}{a} \right)^2 dx dy + \\ &+ \frac{t\sigma_y}{2} \int_0^a \int_0^b \left[\frac{\pi}{b} \left(A_{m1} \cos \frac{\pi y}{b} + 2A_{m2} \cos \frac{2\pi y}{b} \right) \sin \frac{m\pi x}{a} \right]^2 dx dy \\ &= \frac{t\sigma_x}{2} \left\{ \frac{1}{2} b A_{m1}^2 + \frac{1}{2} b A_{m2}^2 - \frac{\beta}{b} \left(A_{m1}^2 \cdot \frac{1}{4} b^2 - A_{m1} A_{m2} \frac{16b^2}{9\pi^2} + A_{m2}^2 \cdot \frac{1}{4} b^2 \right) \right\} \frac{m^2 \pi^2}{a^2} \cdot \frac{1}{2} a + \\ &+ \frac{t\sigma_y}{2} \cdot \frac{\pi^2}{b^2} \left(A_{m1}^2 \cdot \frac{1}{2} b + A_{m2}^2 \cdot \frac{1}{2} b \right) \cdot \frac{1}{2} a \\ &= \frac{t\sigma_x}{2} \cdot \frac{ab}{4} \cdot \frac{m^2 \pi^2}{a^2} \left\{ A_{m1}^2 (1 - 0,5\beta) + \frac{32\beta}{9\pi^2} A_{m1} A_{m2} + A_{m2}^2 (1 - 0,5\beta) \right\} + \\ &\frac{t\sigma_y}{2} \cdot \frac{\pi^2 ab}{4b^2} (A_{m1}^2 + A_{m2}^2) \\ &= \frac{t\sigma_x}{8} \cdot \frac{m^2 \pi^2}{a} \left\{ A_{m1}^2 (1 - 0,5\beta) + \frac{32}{9\pi^2} A_{m1} A_{m2} + A_{m2}^2 (1 - 0,5\beta) \right\} + \frac{t\sigma_y}{8} \pi^2 a (A_{m1}^2 + A_{m2}^2)\end{aligned}$$

Substitution into the equation of the strain energy:

$$I = \frac{1}{2} \int_0^a \int_0^b \left\{ N_x \left(A_{m1} \sin \frac{\pi y}{b} + A_{m2} \sin \frac{2\pi y}{b} \right)^2 \left(\frac{m^2 \pi^2}{a^2} \sin \frac{m\pi x}{a} \right)^2 + \right.$$

$$\begin{aligned}
& + 2N_{xy} \left(A_{m1} \cos \frac{\pi y}{b} + 2A_{m2} \cos \frac{2\pi y}{b} \right)^2 \left(\frac{m\pi^2}{ab} \cos \frac{m\pi x}{a} \right)^2 + \\
& + N_y \left(A_{m1} \sin \frac{\pi y}{b} + 4A_{m2} \sin \frac{2\pi y}{b} \right)^2 \left(\frac{\pi^2}{b^2} \sin \frac{m\pi x}{a} \right)^2 \Big\} dx dy \\
I = & \frac{1}{2} \left\{ N_x (A_{m1}^2 \cdot \frac{1}{2}b + A_{m2}^2 \cdot \frac{1}{2}b) \frac{m^4 \pi^4}{a^4} \cdot \frac{1}{2}a + 2N_{xy} (A_{m1}^2 \cdot \frac{1}{2}b + 4A_{m2}^2 \cdot \frac{1}{2}b) \frac{m^2 \pi^4}{a^2 b^2} \cdot \frac{1}{2}a + \right. \\
& \left. + N_y (A_{m1}^2 \cdot \frac{1}{2}b + 16A_{m2}^2 \cdot \frac{1}{2}b) \frac{\pi^4}{b^4} \cdot \frac{1}{2}a \right\} \\
= & \frac{ab}{8} \left\{ N_x (A_{m1}^2 + A_{m2}^2) \frac{m^4 \pi^4}{a^4} + 2N_{xy} (A_{m1}^2 + 4A_{m2}^2) \frac{m^2 \pi^4}{a^2 b^2} + N_y (A_{m1}^2 + 16A_{m2}^2) \frac{\pi^4}{b^4} \right. \\
= & \frac{m^2 \pi^4}{8ab} \sqrt{N_x N_y} \left[A_{m1}^2 \left\{ \sqrt{\frac{N_x}{N_y}} \left(\frac{m}{\alpha} \right)^2 + \frac{2N_{xy}}{\sqrt{N_x N_y}} + \sqrt{\frac{N_y}{N_x}} \left(\alpha \right)^2 \right\} + \right. \\
& \left. + A_{m2}^2 \left\{ \sqrt{\frac{N_x}{N_y}} \left(\frac{m}{\alpha} \right)^2 + \frac{8N_{xy}}{\sqrt{N_x N_y}} + 16 \sqrt{\frac{N_y}{N_x}} \left(\alpha \right)^2 \right\} \right] \\
= & \frac{m^2 \pi^4}{8ab} \sqrt{N_x N_y} (A_{m1}^2 a_{m1} + A_{m2}^2 a_{m2})
\end{aligned}$$

Now

$$\begin{aligned}
I - U = & \frac{\pi^4 m^2}{8ab} \sqrt{N_x N_y} \left[A_{m1}^2 \left\{ a_{m1} - \frac{t\sigma_x \cdot b^2}{\pi^2 \sqrt{N_x N_y}} (1 - 0,5\beta) - \frac{t\sigma_y a^2}{m^2 \pi^2 \sqrt{N_x N_y}} \right\} + \right. \\
& \left. - 2A_{m1} A_{m2} \cdot \frac{16t\sigma_x \beta b^2}{9\pi^4 \sqrt{N_x N_y}} + A_{m2}^2 \left\{ a_{m2} - \frac{t\sigma_x b^2}{\pi^2 \sqrt{N_x N_y}} (1 - 0,5\beta) - \frac{t\sigma_y a^2}{m^2 \pi^2 \sqrt{N_x N_y}} \right\} \right]
\end{aligned}$$

Differentiation with respect to A_{m1} and A_{m2} gives:

$$\begin{aligned}
A_{m1} \{ a_{m1} - \lambda_1 (1 - 0,5\beta) - \lambda_2 \} - A_{m2} \frac{16\lambda_1 \beta}{9\pi^2} & = 0 \\
-A_{m1} \frac{16\lambda_1 \beta}{9\pi^2} + A_{m2} \{ a_{m2} - \lambda_1 (1 - 0,5\beta) - \lambda_2 \} & = 0
\end{aligned}$$

in which

$$\lambda_1 = \frac{t\sigma_x b^2}{\pi^2 \sqrt{N_x N_y}} \quad \text{and} \quad \lambda_2 = \frac{t\sigma_y a^2}{m^2 \pi^2 \sqrt{N_x N_y}}$$

The solution of these two equation can be found by equating the determinant to zero.
Thus:

$$\{a_{m1} - \lambda_1(1-0,5\beta) - \lambda_2\} \{a_{m2} - \lambda_1(1-0,5\beta) - \lambda_2\} - \left(\frac{16\lambda_1\beta}{9\pi^2}\right)^2 = 0$$

For the case where σ_x and σ_y vary but maintain a constant ratio:

$$\sigma_x = \xi \quad \text{and} \quad \sigma_y = \varphi \cdot \xi$$

then

$$\lambda_2 = \lambda_1 \cdot \varphi \cdot \frac{a^2}{m^2}$$

The critical value of ξ is now:

$$\xi_{cr} = \frac{4\pi^2 \sqrt{N_x N_y}}{tb^2} \times \frac{(a_{m1} + a_{m2}) \left(1 - 0,5\beta + \varphi \frac{a^2}{m^2}\right) + \sqrt{\left(1 - 0,5\beta + \varphi \frac{a^2}{m^2}\right)^2 (a_{m1} - a_{m2})^2 + a_{m1} a_{m2} \left(\frac{32\beta}{9\pi^2}\right)^2}}{8 \left\{ \left(1 - 0,5\beta + \varphi \frac{a^2}{m^2}\right)^2 - \left(\frac{16\beta}{9\pi^2}\right)^2 \right\}}$$

The buckling factor K_p becomes

$$K = \frac{(a_{m1} + a_{m2}) \left(1 - 0,5\beta + \varphi \frac{a^2}{m^2}\right) + \sqrt{\left(1 - 0,5\beta + \varphi \frac{a^2}{m^2}\right)^2 (a_{m1} - a_{m2})^2 + a_{m1} a_{m2} \left(\frac{32\beta}{9\pi^2}\right)^2}}{8 \left\{ \left(1 - 0,5\beta + \varphi \frac{a^2}{m^2}\right)^2 - \left(\frac{16\beta}{9\pi^2}\right)^2 \right\}}$$

In Figs. 5, 6, 7 and 8 combinations of $\sigma'_{xcr}/\sigma_{xcr}$ and $\sigma'_{ycr}/\sigma_{ycr}$ are given for various values of φ , w , α and β . It can be seen that for $m = 1$ relation (6) $\sigma'_{xcr}/\sigma_{xcr} + \sigma'_{ycr}/\sigma_{ycr} = 1$ is a good approximation. For other values of m relation (6) is safe.

In Figs. 9 up to 12 "festoon" curves for K are given for different values of β , φ and w (omega in the diagrams).

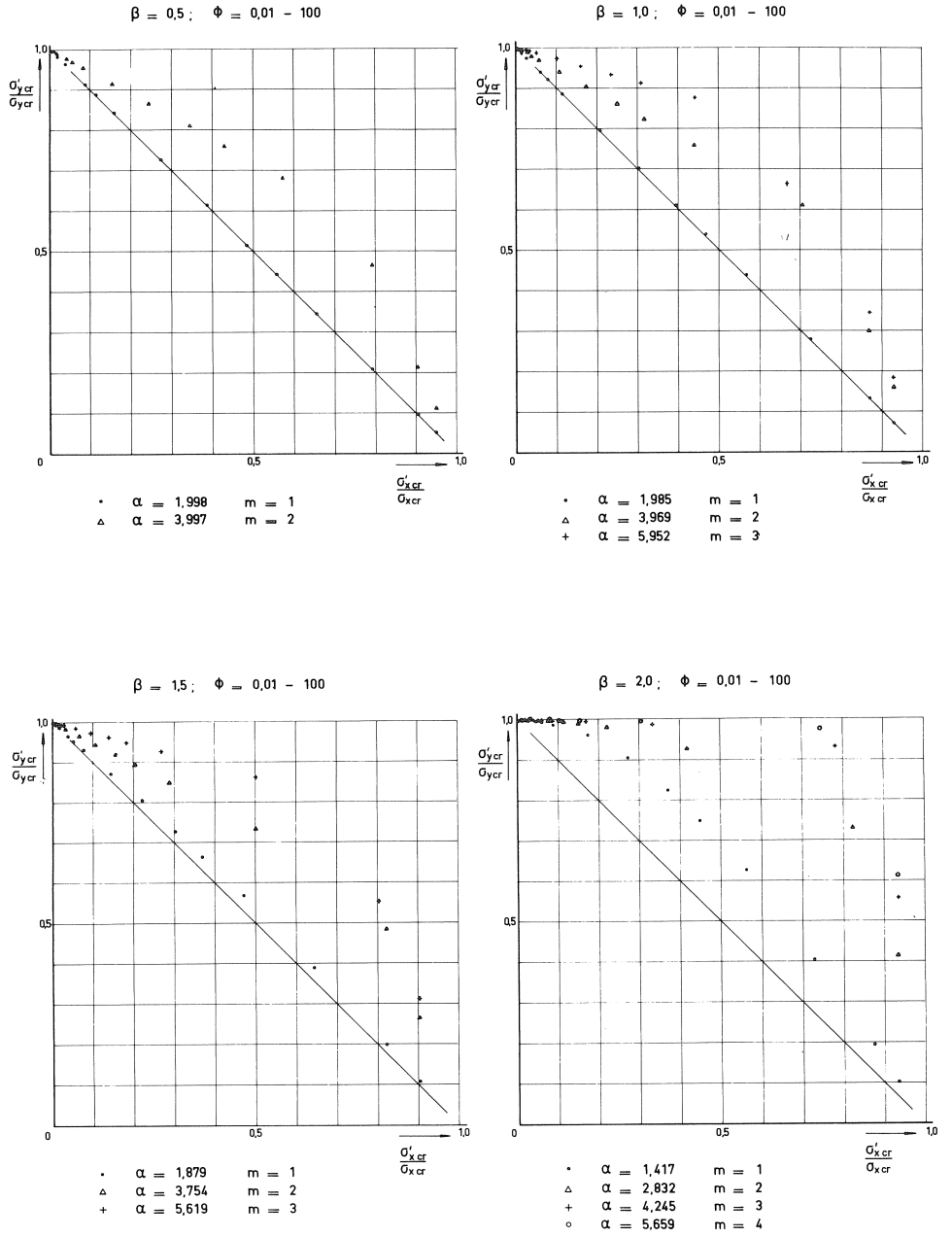


Fig. 5. Relation $\sigma'_{xcr}/\sigma_{xcr}$ and $\sigma'_{ycr}/\sigma_{ycr}$ for $w=0,50$ various values of α, β and ϕ .

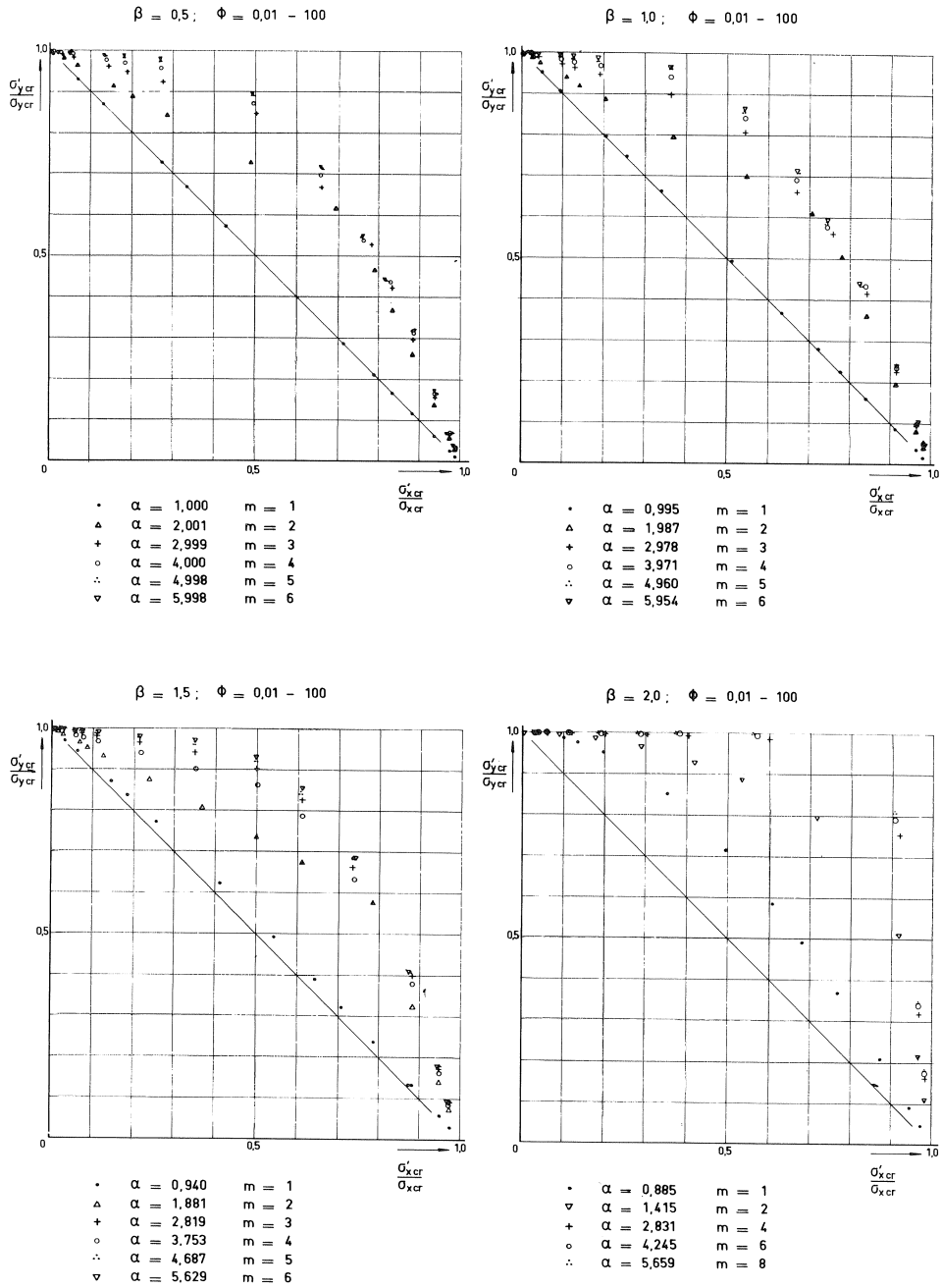


Fig. 6. Relation $\sigma'_{xcr}/\sigma_{xcr}$ and $\sigma'_{ycr}/\sigma_{ycr}$ for $w=1,00$ and various values of α, β and ϕ .

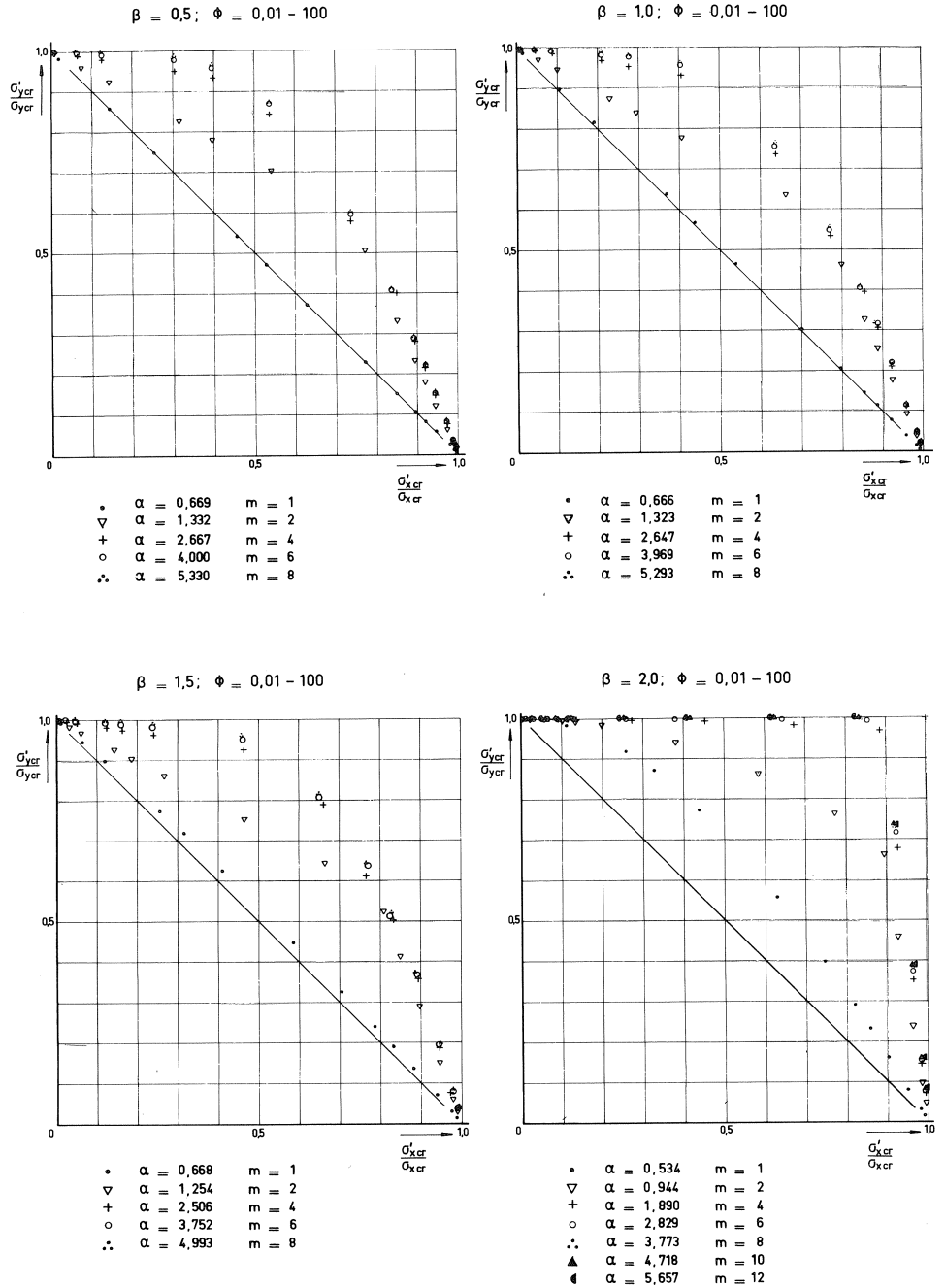


Fig. 7. Relation $\sigma'_{xcr}/\sigma_{xcr}$ and $\sigma'_{ycr}/\sigma_{ycr}$ for $w=1,50$ and various values of α, β and ϕ .

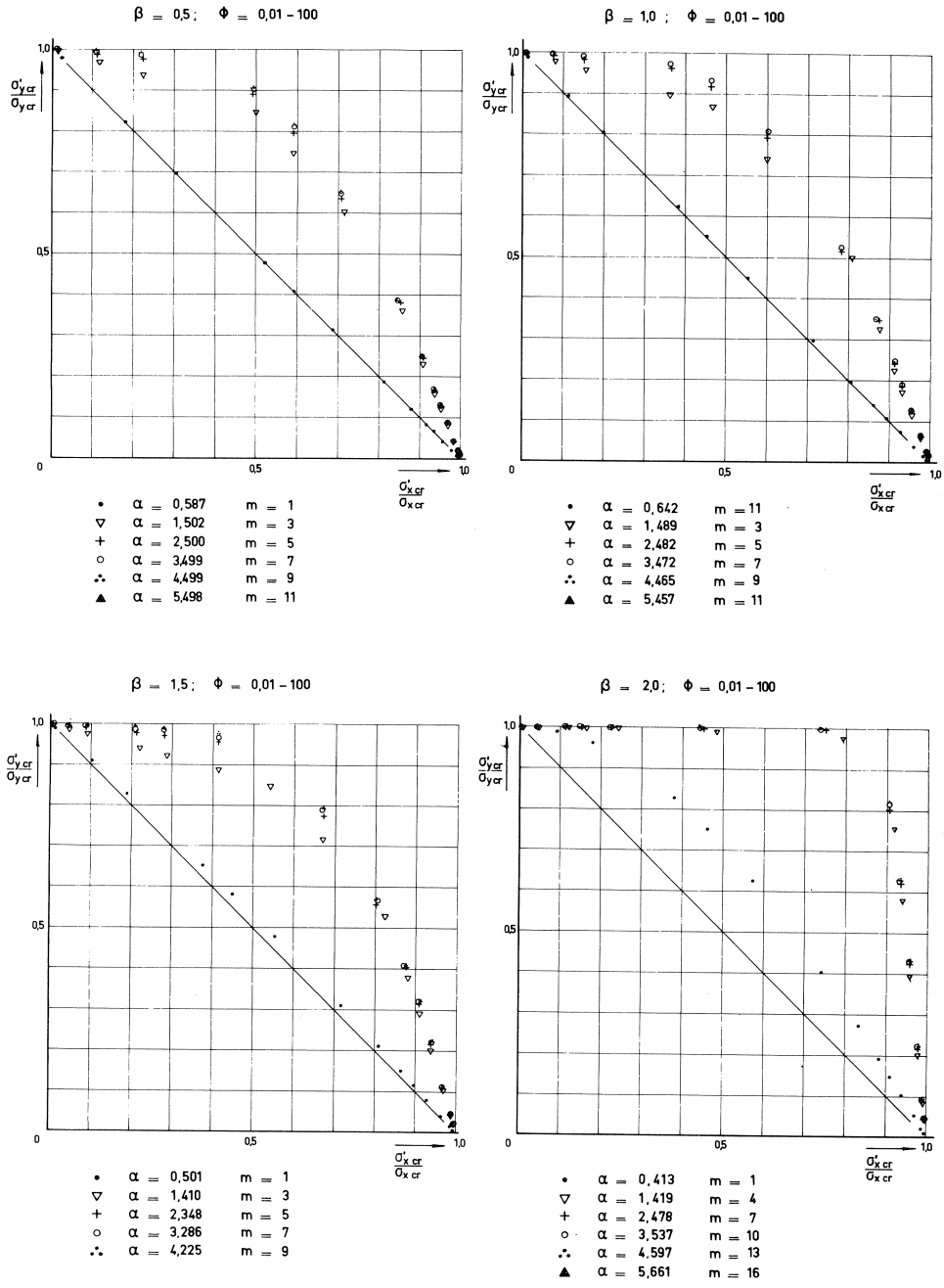


Fig. 8. Relation $\sigma'_{xcr}/\sigma_{xcr}$ and $\sigma'_{ycr}/\sigma_{ycr}$ for $w=2,00$ and various values of α, β and ϕ .

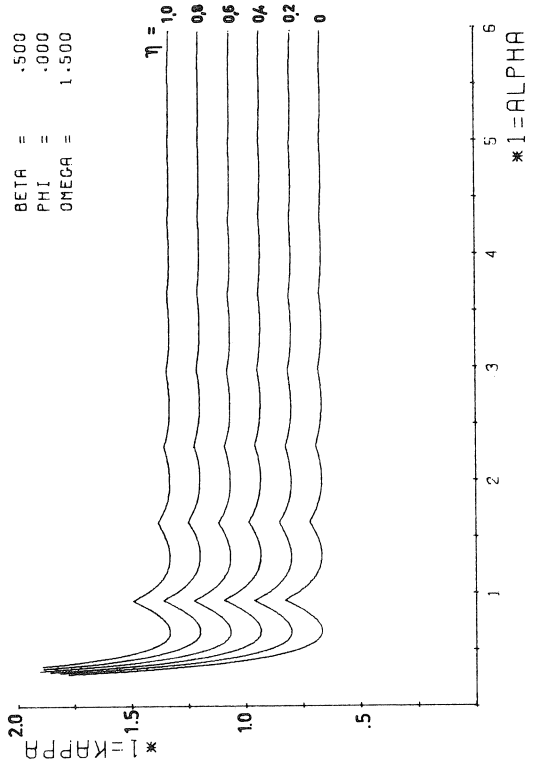
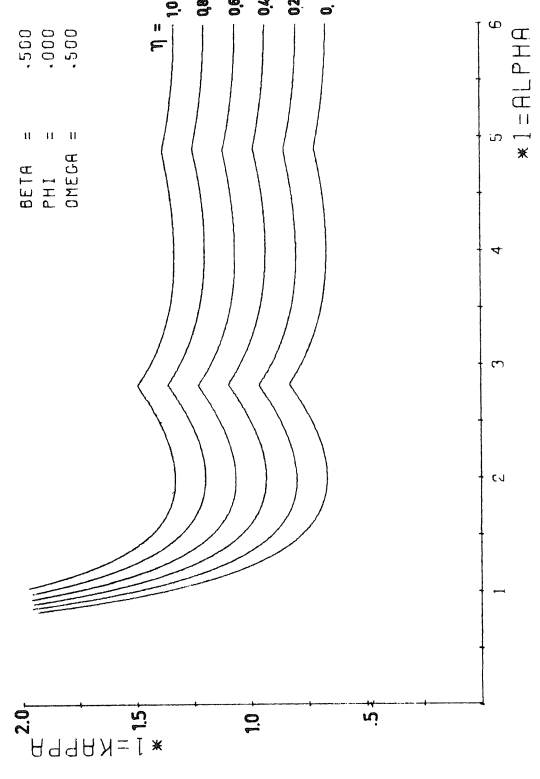
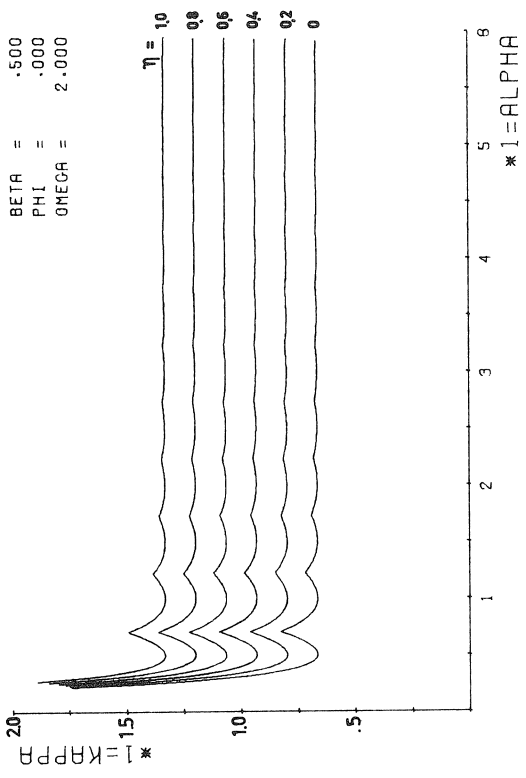
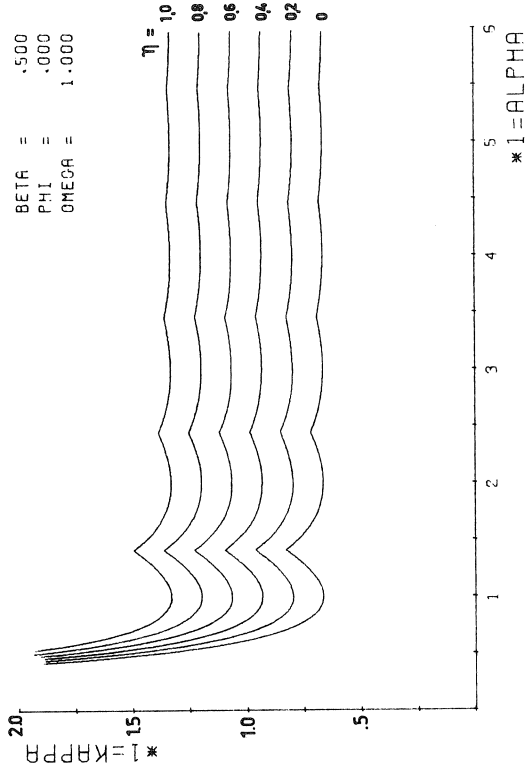


Fig. 9.

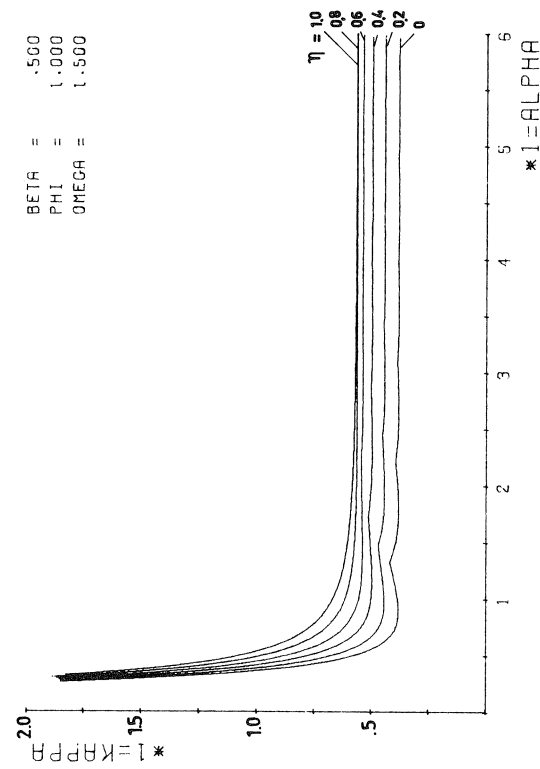
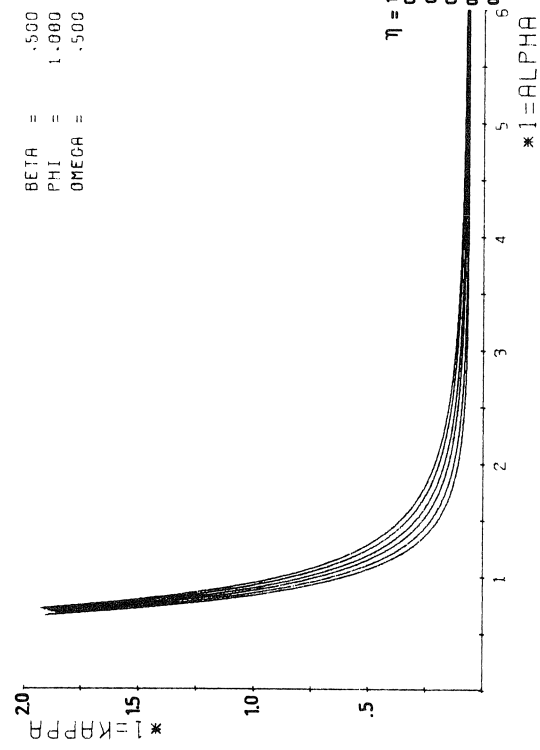
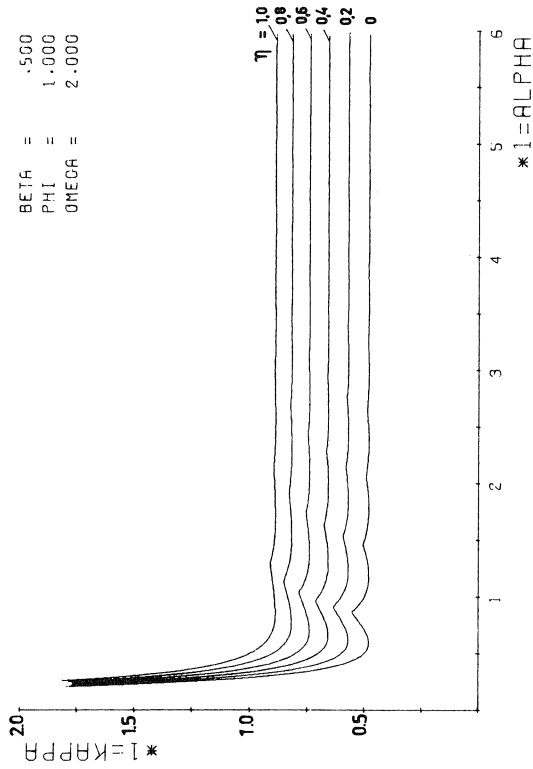
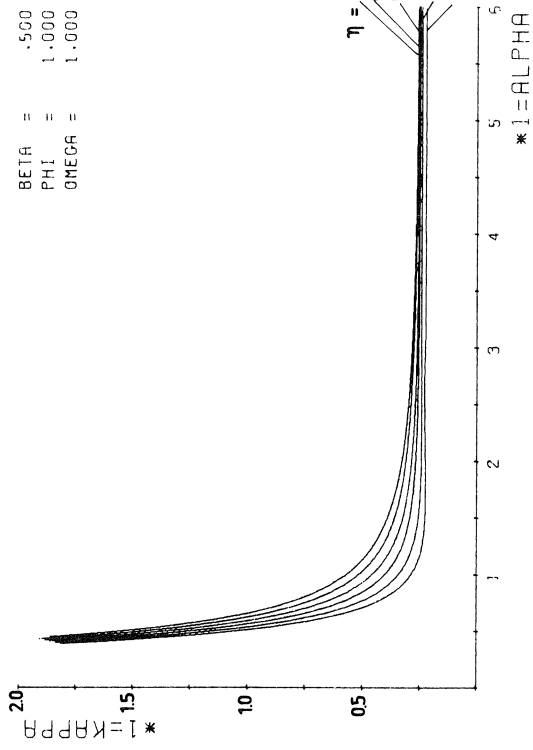


Fig. 10.

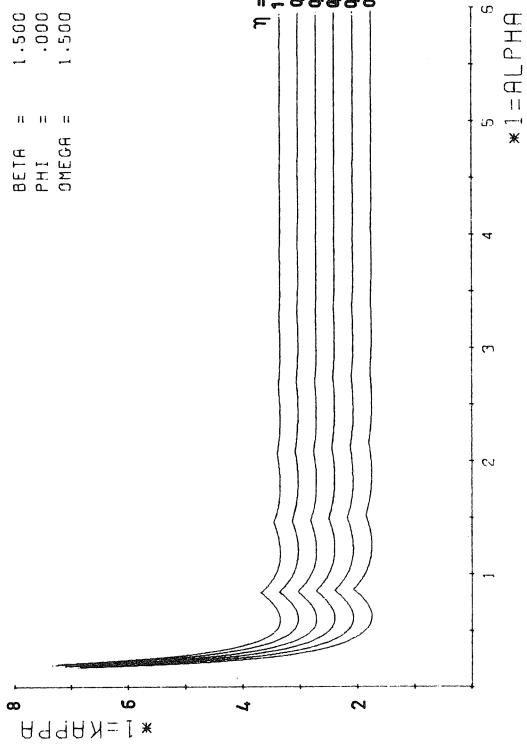
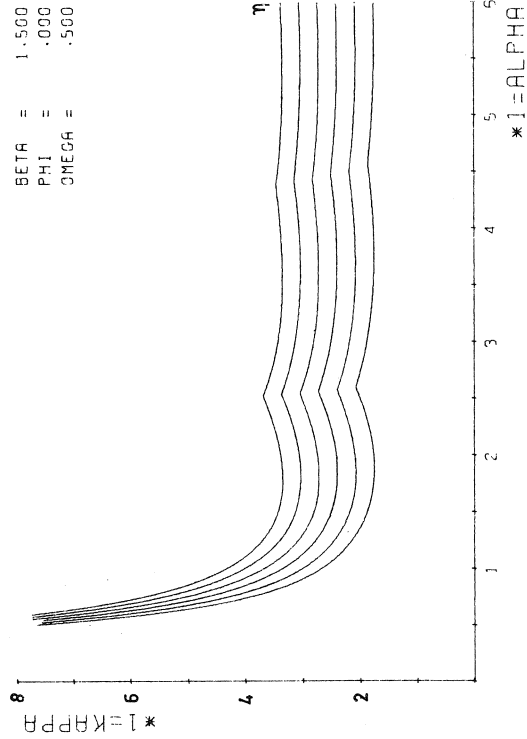
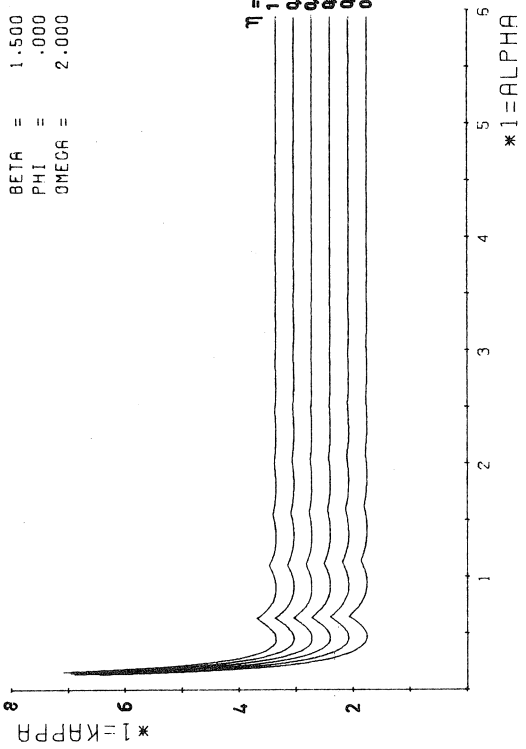
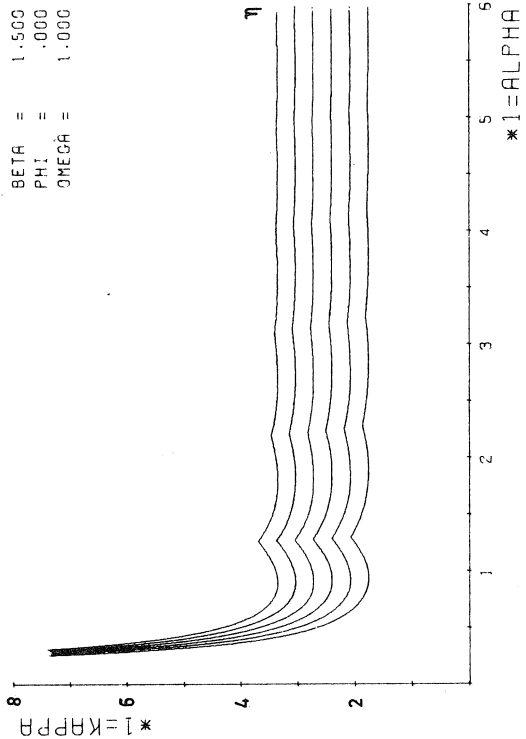
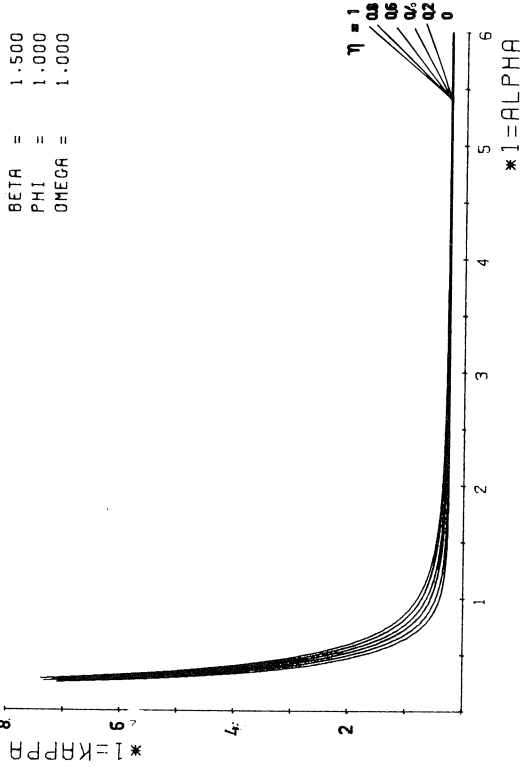
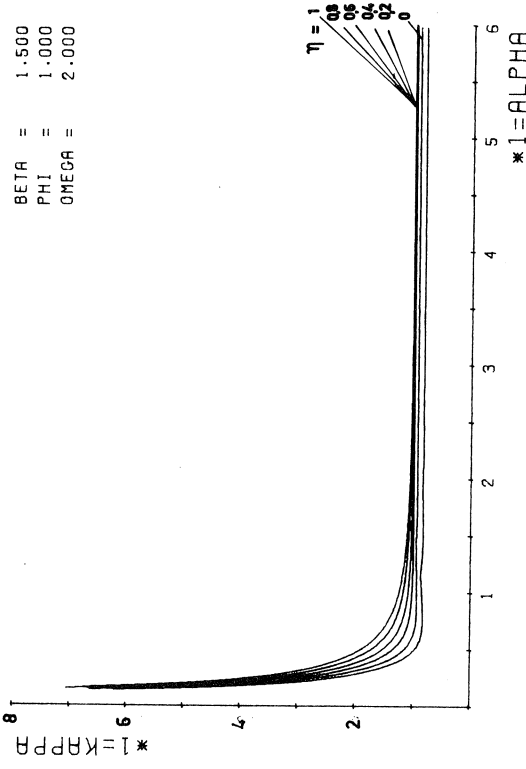


Fig. 11.

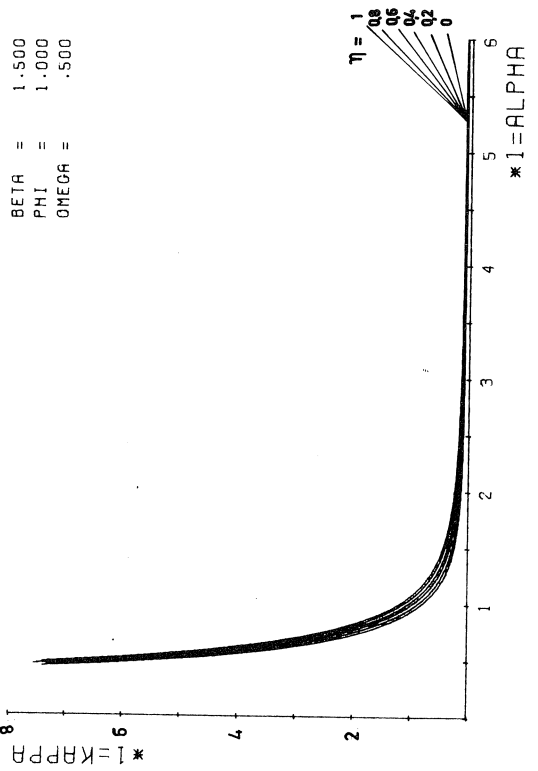
BETA = 1.500
 PHI = 1.000
 OMEGA = 1.000



BETA = 1.500
 PHI = 1.000
 OMEGA = 2.000



BETA = 1.500
 PHI = 1.000
 OMEGA = .500



BETA = 1.500
 PHI = 1.000
 OMEGA = 1.500

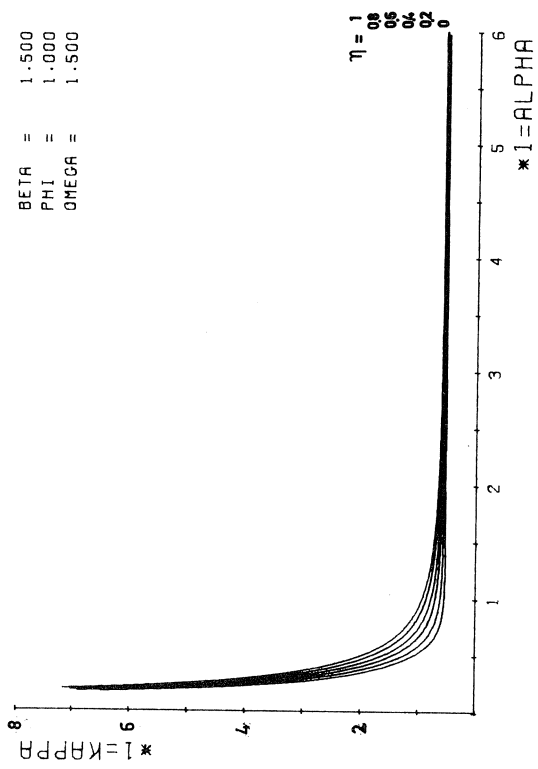


Fig. 12.